The effect of aspect ratio in counter-current gas-liquid bubble columns: Experimental results and gas holdup correlations

Giorgio Besagni *, Alessandro Di Pasquali, Lorenzo Gallazzini, Elia Gottardi, Luigi Pietro Maria Colombo, Fabio Inzoli

Politecnico di Milano, Department of Energy, Via Lambruschini 4a, 20156, Milano

It is generally admitted that the gas holdup is independent of the column dimensions and gas sparger design if three criteria are satisfied: the diameter of the bubble column is larger than 0.15 m, gas sparger openings are larger than 1–2 mm and the aspect ratio is larger than 5. This paper contributes to the ex- isting discussion; in particular, the effect of the aspect ratio (within the range 1–15) in a counter-current gas-liquid bubble column has been experimentally studied and a new gas holdup correlation to estimate the influence of aspect ratio, operation mode and working fluid on the gas holdup has been proposed. The bubble column, equipped with a spider gas sparger, is 5.3 m in height, has an inner diameter of 0.24 m; gas superficial velocities in the range of 0.004–0.23 m/s have been considered, and, for the runs with water moving counter-currently to the gas phase, the liquid has been recirculated at a superficial velocity of −0.0846 m/s. Filtered air has been used as the gaseous phase in all the experiments, while the liquid phase has included tap water and different aqueous solutions of sodium chloride as electrolyte. Gas holdup measurements have been used to investigate the flow regime transitions and the global bubble column hydrodynamics. The counter-current mode has turned out to increase the gas holdup and destabi- lize the homogeneous flow regime; the presence of electrolytes has resulted in increasing the gas holdup and stabilizing the homogeneous flow regime; the aspect ratio, up to a critical value, has turned out to decrease the gas holdup and destabilize the homogeneous flow regime. The critical value of the aspect ratio ranged between 5 and 10, depending on the bubble column operation (i.e., batch or counter-current modes) and liquid phase properties. Since no correlation has been found in the literature that can cor- rectly predict the gas holdup under the investigated conditions, a new scheme of gas holdup correlation has been proposed. Starting from considerations concerning the flow regime transition, corrective param- eters are included in the gas holdup correlation to account for the effect of the changes introduced by the aspect ratio, operation mode and working fluid. The proposed correlation has been found to predict fairly well the present experimental data as well as previously published gas holdup data.

Keywords: Bubble column, Gas holdup, Flow regime transitions, Counter-current mode, Electrolyte, Gas holdup correlation

1. Introduction

Bubble columns are multiphase reactors where a gas phase is dispersed into a continuous phase (i.e., a liquid phase—two-phase bubble column: the subject of this study—or a suspension—slurry bubble column) in the form of "*non-coalescence-induced*"/disperse bubbles or of "*coalescence-induced*" bubbles. The two-phases are separated by an interface between the dispersed phase and the continuous phase; at this interface, interfacial transport phenomena (i.e., heat and mass transfer) may occur. Two-phase bubble columns are widely used in chemical, petrochemical and biochemical industries thanks to the many advantages they provide in both design and operation. On the practical point of view, the simplicity of construction, the lack of any mechanically operated parts, the low energy input requirements, the large contact area between the liquid and gas phases, and the good mixing within the liquid phase are some of the practical advantages in bubble column technology. The simplest bubble column configuration consists in a vertical cylinder with no internals, in which the gas phase enters at the bottom—through a gas sparger—and the liquid phase is supplied in batch mode or it may be led in either co-currently or counter-currently to the upward gas stream. Eventually, internal devices may be added to control the heat transfer, to limit the liquid phase back-mixing or to foster the bubble break-up rate (as reviewed in ref. Youssef Ahmed et al., 2013). These elements have significant effects on the fluid dynamics inside the reactor and the prediction of these effects is still hardly possible without experimenta-

Article history:
Received 19 September 2016
Revised 2 March 2017
Accepted 19 April 2017
Available online 21 April 2017

* Corresponding author.
E-mail address: giorgio.besagni@polimi.it (G. Besagni).

Published Journal Article available at: http://dx.doi.org/10.1016/j.ijmultiphaseflow.2017.04.015

Nomenclature

Symbols

a	Yardstick resolution [m]
A_c	Cross-sectional area of the bubble column [m^2]
A_i $(i=1,2)$	Parameters in the gas holdup correlation (Eq. (21)) [-]
B	Retarded Hamaker constant (Eq. (2)) [J m]
C_0	Distribution parameter (Eq. (15)) [-]
C_i $(i=1,2,3,4,5,6,7)$	Parameters in the gas holdup correlations (Eqs. (24) and (33)) [-]
d_o	Gas sparger holes diameter [mm]
d_c	Diameter of the column [m]
D_H	Hydraulic diameter [m]
D^*_H	Non-dimensional diameter (Eq. (1)) [-]
error	Relative error (Eq. (25))[-]
g	Acceleration due to gravity [m/s^2]
H_c	Height of the column [m]
H_D	Height of the free-surface after aeration [m]
H_0	Height of the free-surface before aeration [m]
l	Number of additional measurements in uncertainty evaluation [-]
J	Drift-flux [m/s]
n	Molar concentration of NaCl [mol/l]
n_t	Molar transition concentration of NaCl (Eq. (2)) [mol/l]
n^*	Dimensionless concentration (Eq. (2)) [-]
Ndata	Total number of data in the dataset, in MPE and MAPE evaluation (Eqs.(27) and (28)) [-]
o	Exponent in the drift-flux method (Eqs. (13) and (14)) [m/s]
Q	Volumetric flow rate [m^3/s]
r_b	Bubble radius (Eq. (2)) [mm]
R_g	Gas constant (Eq. (2)) [J /K mol]
s_H	Sample standard deviation of a measurement [m]
S_i $(i=1,2,3)$	Parameters in the swarm velocity method (Eq. (8)) [-]
T	Temperature [K]
u_d	Weighted mean drift velocity (Eq. (15)) [m/s]
u_g	Mean rise velocity of the gas phase [m/s]
U_b	Parameter in the drift-flux method (Eq. (11)) [m/s]
U_∞	Terminal velocity of an isolated bubble (Eqs. (13) and (14)) [m/s]
U	Superficial velocity [m/s]
U^*	Dimensionless velocity (Eq. (24)) [-]
u	Mean rise velocity of the gas phase [m/s]
v	Bubble terminal velocity [m/s]
V	Volume [m^3]
w	Local phase velocity [m/s]
$w_{G\text{-}L}$	relative velocity between the phases (Eq. (B.12)) [m/s]
$w_{G->L}$	drift velocities (Eqs. (B.13) and (B.14)) [m/s]

Greek Symbols

μ	Viscosity [N s/m^2]
β	Exponent (Eq. (18)) [-]
γ	Parameter in the counter-current gas holdup correlation (Eq. (29)) [-]
ε	Holdup [-]
ρ	Density [kg/m^3]
σ	Surface tension [N/m]
ξ_{H0}	Uncertainty related to the evaluation of H_0 (Eq. (A.1)) [m]

Subscripts

Batch	Batch mode
c	Bubble column parameter
Correlation	Value obtained from correlation
Counter-current	Counter-current mode
Cr	Critical value
Experimental	Experimental value
G	Gas phase
Homogeneous	Homogeneous flow regime
i	Data considered in the dataset, in MPE and MAPE evaluation (Eqs. (27) and (28))
I	First flow regime transition point
II	Second flow regime transition point
L	Liquid phase
Slug-bubble	Slug-bubble parameter
Swarm	Swarm velocity
T, E	Subscripts in the drift-flux formulation (Eqs. (10)–(12), (14))
Trans	Flow regime transition point
Transition	Transition flow regime
Wallis	Wallis plot method
Wt	Mass concentration
Zuber-Finley	Zuber-Finley method

Superscripts

R1	Homogeneous flow regime (Eq. (22))
R2	Heterogeneous flow regime (Eq. (22))

Acronyms

MPE	mean percentage error (Eq. (27))
MAPE	Mean absolute percentage error (Eq. (28))
AR	Aspect ratio ($AR=H_0/d_c$)
BSD	Bubble size distribution
Fr	Froude number ($Fr=U_G/(gH_0)$)
NaCl	Sodium chloride

Other

Batch mode	$U_L=0$
Counter-current mode	$U_L<0$
||	Consider only the numerical value without units
	Mean value

tion. It is worth noting that the mass transfer that takes place at the interface does not necessarily involve reactions between gas and liquid components, even if this occurs in many practical cases (i.e., oxidation, hydrogenation, chlorination, phosgenation and alkylation processes). Despite the simple bubble column design, complex fluid dynamics interactions and coupling between the phases (which manifests in the prevailing flow regimes (Majumder, 2016)) exist; please note the fluid dynamics in bubble columns is similar to the ones observed in nuclear and energy conversion systems. Therefore, correct design and operation of bubble column reactors rely on the proper prediction of the global and local fluid dynamic properties: a typical approach is apply scale-up methods to estimate the fluid dynamics of "*industrial-reactor-scale*" reactors from "*laboratory-reactor-scale*" experimental facilities (Shaikh and Al-Dahhan, 2013). Subsequently, models for the interfacial mass

transfer (Rzehak, 2016) and, eventually, to take into account the multi-phase reactions, are applied. Among the many fluid dynamic properties, the gas holdup (ε_G)—a dimensionless parameter defined as the volume of the gas phase divided by the total volume of the system—is a global fluid dynamic property of fundamental and practical importance. The gas holdup determines the mean residence time of the dispersed phase and, in combination with the size distribution of the dispersed phase, the interfacial area for the rate of interfacial heat and mass transfer. The global and the local fluid dynamic properties depend on the many variables of the systems (i.e., the operation mode, the physical properties of the phases, the properties at the gas-liquid interface, …) and are related to the prevailing flow regime, which can be distinguished— in a large-diameter column—in (a) the homogeneous flow regime, (b) the transition flow regime and (c) the heterogeneous flow regime (see the discussions in ref. Besagni and Inzoli., 2016c and Besagni et al., 2016b, 2017). The scale-up approaches from the "*laboratory-reactor-scale*" towards the "*industrial-reactor-scale*" rely on similarity criteria that would result in similar mixing and fluid dynamics and, hence, transport and performance in the two different scales. Many approaches were proposed and, in this respect, a pioneering study was proposed by Wilkinson et al. (1992), after performing experiments in two different column diameters ($d_c = 0.15$ and $d_c = 0.23$ m), at different operating pressures and using different liquid phases (n-heptane, monoethylene glycol, and water). Based on their own results as well as on literature data, they concluded that the gas holdup is independent of the column dimensions and the gas sparger design if the following criteria (the "*Wilkison* et al. *scale-up criteria*") are satisfied[1]:

1. **criterion 1.** The diameter of the bubble column, d_c, is larger than 0.15 m;
2. **criterion 2.** The aspect ratio, *AR* (the ratio between the height and the diameter of the column), is larger than 5;
3. **criterion 3**. The gas sparger openings diameter, d_o, is larger than 1–2 mm ("*coarse*" gas spargers).

The discussion concerning the large-diameter effects (criterion 1) was proposed in our previous papers (i.e., Besagni and Inzoli, 2016b,c; Besagni et al., 2017 – see Section 2.1.1) and the influence of the gas sparger design (criterion 2) a matter of ongoing research activities (and is to be presented elsewhere). This paper contributes to the existing discussion and mainly focuses on the influence of the aspect ratio, *AR*, in gas-liquid large-diameter bubble columns (criterion 3). It is worth noting that, despite some authors defined the aspect ratio in terms of the column height H_c, the correct definition of *AR* strictly relies on the initial liquid level ($AR = H_0/d_c$), rather the column height, as discussed by Sasaki et al. (2016,2017) and demonstrated in this study. Generally speaking, in the systems where the bubble sizes are not at their maximum equilibrium size[2] (and where coalescence may occur), the liquid height will influence the extent of the coalescence. Consequently, the gas holdup would decrease with the liquid height, because the higher the column the longer the time the bubbles have to coalesce and, thus, the lower the mean residence time of the gas phase. Furthermore, in shorter bubble columns, the liquid circulation patterns (that tends to decrease the gas holdup) are not fully developed and the end-effects (i.e., near gas sparger and top-column effects) are more evident; actually, Xue et al. (2008) found a strong influence of the gas sparger properties in the local void fractions up to $AR = 5$. All these phenomena (namely, coalescence, local flow phenomena and gas sparger effects) tend to destabilize the homogeneous flow regime in shorter bubble columns. The number of studies dealing with the influence of the liquid level (*AR*) on the bubble column fluid dynamics is quite limited and, in the following, a literature survey is proposed. All the details of the studies listed below (i.e., bubble column and gas sparger design), along with other studies that will be used in the following to compare our experimental data, are summarized in Table 1 (refs. Akita and Yoshida, 1973; Patil et al., 1984; Reilly et al., 1986; Rollbusch et al., 2015a; Ruzicka et al., 2001a; Sarrafi et al., 1999; Sasaki et al., 2016; Sasaki et al., 2017; Schumpe and Grund, 1986; Thorat et al., 1998; Wilkinson et al., 1992; Yoshida and Akita, 1965; Zahradník et al., 1997). In one of the very first study, Yoshida and Akita (1965) did not observed any remarkable effects of *AR* on the gas holdup and mass transfer in their experiments; it is worth noting that they also studied a small-diameter bubble column. Patil et al. (1984), using a "*very coarse*" gas sparger (a pure heterogeneous flow regime is expected), did not observed any remarkable effect of *AR* on the gas holdup. Later, Wilkinson et al. (1992)—when presenting the "*Wilkison* et al. *scale-up criteria*" —discussed the results obtained by Kastanek et al. (1984): the influence of *AR* is negligible for H_C greater than 1–3 m and with *AR* larger than 5. (Zahradník et al., 1997) found that the gas holdup decreases and the homogeneous flow regime is destabilized while increasing the initial liquid level up to a critical aspect ratio, AR_{Cr}; the authors concluded that their results support the assumption of a negligible influence of *AR* on gas holdup and flow regime transitions for *AR* larger than 5. These assumption has been also confirmed by Thorat et al. (1998), which found a negligible influence of *AR* on the gas holdup for *AR* larger than 5 (air-water system) or 8 ("*non-coalescing*" system). Sarrafi et al. (1999) compared their experimental results with other experimental data and excluded any effect of the initial liquid level on the flow regime transition, for $H_0 > 3$ m. Ruzicka et al. (2001a) found that an increase in liquid height destabilizes the homogeneous flow regime and decreases the gas holdup up to critical values. Sasaki et al. (2016) found that an increase in liquid height destabilizes the homogeneous flow regime and decreases the gas holdup up (*AR* up to 5); in addition, they proposed the very first gas holdup correlation taking into account H_0. More recently, Sasaki et al. (2017) further developed their previous work (Sasaki et al., 2016) and studied large-diameter bubble columns at low-intermediate *AR* (d_C in the range of 0.16–0.3 m - *AR* up to 6.5) and very-large-diameter bubble column at low *AR* ($d_C = 2$ m - *AR* up to 2). They concluded that the gas holdup is independent of the column design in large-diameter and high *AR* bubble column; in particular, they stated as follows: "*the effects of* d_c *and* H_0 *on* ε_G *are negligible when scaling up from small to large bubble columns, provided that* α_G *in the small columns are obtained for* $d_C \geqslant 200$ *mm and* $H_0 \gtrsim 2200$ *mm. The height-to-diameter ratio is useless in evaluation of the critical height, above which* ε_G *does not depend on* H_0." (Please notice that the nomenclature has been changed accordingly with our notation list). This conclusion is quite interesting and, at present, this is the only study with tends to disagree on the concept of *AR* as scale-up criterion. This topic is further considered in the following of the paper and our point of view is stated in outlook sections. From the literature survey, it is clear that there is a lack of studies concerning:

[1] These three criteria are the rule of the thumb in bubble column scale-up. To the authors' opinion, all these criteria can be expressed in term of non-dimensional groups: (a) non-dimensional diameter (i.e., Eq. (1)); (b) non-dimensional dimension of the bubble column (i.e., the aspect ratio, AR); (c) non-dimensional sparger opening. This concept is a matter of ongoing research and it will be formalized in future works. The present paper is intended as a first step towards the study of these criteria, with a major focus on the aspect ratio.

[2] This situation is typical of bubble columns with "*coarse*" spargers (i.e., ring or spider spargers, $d_o > 1$–1.5 mm): large sparger openings generally produce a non-stable bubble size distribution at the inlet, which evolves, in the axial direction of the bubble column, towards an equilibrium. Conversely, when using "*fine*" gas spargers (having small gas sparger openings $d_o < 0.5$–1 mm), the bubble bed produced by the gas sparger may be stable from the beginning. A stable bubble bed at the inlet may change the relationship between the gas holdup and superficial gas velocity (i.e., the gas holdup curve is "*S-shaped*") and may stabilize the homogeneous flow regime.

1. the influence of *AR* for (a) the different operation modes of a bubble column (i.e., batch and counter-current) and (b) the different liquid phase properties (i.e., non-coalescing systems);
2. the influence of *AR* on (a) the gas holdup and (b) the two flow regime transitions existing in large-diameter columns (the homogeneous/transition and the transition/heterogeneous flow regime transitions);
3. gas holdup correlations taking into account (a) *AR*, (b) the operation mode and (c) the liquid phase properties (i.e., the only correlation taking into account H_0 is the one proposed by Sasaki et al., 2016 and one of the few attempts to obtain counter-current correlations has been previously presented by the authors De Guido et al., 2016).

Taking into account the above-mentioned gaps in the literature, the goal of this study is to understand the influence of the column aspect ratio and to contribute to the existing discussion on the scale-up criteria for multiphase reactors. In this respect, this paper may propose an original point of view on the scale-up criteria, which is in line with the goals of a very recent study proposed by Sasaki et al. (2017) concerning the role of bubble column diameter and initial liquid level. In particular, in this paper, we have studied the effect of *AR* in a counter-current gas-liquid bubble column and we have proposed a gas holdup correlation to estimate the influence of aspect ratio, operation mode and working fluid on the gas holdup. The bubble column, equipped with a spider gas sparger, is 5.3 m in height, has an inner diameter of 0.24 m, we have considered gas superficial velocities in the range of 0.004–0.23 m/s, and, for the runs with water moving counter-currently to the gas phase, the liquid has been recirculated at a superficial velocity of −0.0846 m/s. Filtered air has been used as the gaseous phase in all the experiments, while the liquid phase has included tap water and different aqueous solutions of sodium chloride (NaCl) in the "*coalescent flow regime*" and "*non-coalescent flow regime*", as discussed by Besagni and Inzoli (2015, 2016c). The experimental investigation has consisted in gas holdup measurements, which has been used to investigate the flow regime transitions and the global bubble column fluid dynamics. Moreover, a new correlation for the gas holdup has been developed reaching a satisfactory accuracy in an extended range of conditions: the proposed correlation takes into account the operation mode, the liquid phase properties and the aspect ratio.

The paper is organized as follows. The experimental setup and methods are described in Section 2. The experimental results are presented and discussed in Section 3 and are used to develop a correlation for the gas holdup in Section 4. Finally, the main conclusions, outcomes and outlooks of this study are discussed.

2. The experimental setup and methods

2.1. Experimental setup and liquid phases

2.1.1. Experimental setup

The experimental facility (Fig. 1a), available at the Department of Energy of Politecnico di Milano, is a non-pressurized vertical pipe made of Plexiglas® with $d_c = 0.24$ m and $H_c = 5.3$ m. The column diameter classifies this facility as a large-diameter bubble column. The classification of large-diameter bubble column, is related to the fluid dynamic properties of the bubble columns itself and, in particular, it is related to the absence of the slug flow regime because of the Rayleigh–Taylor instabilities (see ref. Kitscha and Kocamustafaogullari, 1989). The quantification of the Rayleigh–Taylor instabilities at the "*reactor-scale*" is quantified through the dimensionless diameter D^*_H, which is related to the Eötvös number of the slug bubbles as follows (See ref. Besagni and Inzoli, 2016b; Besagni et al., 2017):

$$D^*_H = \frac{D_H}{\sqrt{\sigma/g(\rho_L-\rho_G)}} \xrightarrow{Circular\ bubble\ column} \frac{d_c}{\sqrt{\sigma/g(\rho_L-\rho_G)}} = \\ = \frac{1}{\sqrt{\sigma/d_c^2 g(\rho_L-\rho_G)}} = \frac{1}{\sqrt{1/Eo_c}} = \sqrt{Eo_c} = \sqrt{Eo_{slug-bubble}} \quad (1)$$

In Eq. (1), D_H is the hydraulic diameter, d_c is the bubble column (inner) diameter, σ is the surface tension, g is the acceleration due to gravity, ρ_L - ρ_G is the density difference between the two phases, and $Eo_c = Eo_{slug\text{-}bubble}$ is the Eötvös number computed using the bubble column diameter, which is also the characteristic length of the slug bubbles. Bubble columns with D^*_H greater than the critical value $D^*_{H,cr} = 52$ (accordingly with Brooks et al., 2012)—corresponding to $Eo_{slug\text{-}bubble} = 7.21$ (i.e., $d_c \gtrsim 0.13$–0.15 m; ambient temperature and pressure)—are considered to be large-diameter bubble columns. When the $d_c > D^*_{H,cr}$, the cap bubbles can no more be sustained, and "*coalescence-induced*" bubbles (or, cluster of bubbles) appear instead of the slug flow regime.[3] The present bubble column has a dimensionless diameter $D^*_H = 88.13$ (Besagni and Inzoli, 2016b). When the column diameter is larger than the critical value, the stabilizing effect of the channel wall on the interface of the Taylor bubbles decreases, and slug flow cannot be sustained anymore because of the Rayleigh–Taylor instabilities. The fluid dynamic properties in large-diameter columns differ from the flow in small-diameter columns and the flow regime maps and flow regime transition criteria used to predict the behavior of two-phase flow in small-diameter columns may not be scaled up to understand and predict the flow in large ones (Shawkat and Ching, 2011), in agreement with the scale-up criteria of Wilkinson et al. (1992) and the flow map of Shah et al. (1982). The large diameter effects were described in our previous paper, to whom the reader may refer (for example, refs. Besagni et al., 2016a; Besagni and Inzoli, 2016b, c)

In the experimental facility (Fig. 1a), a pressure reducer controls the pressure upstream from the rotameters (1) and (2), used to measure the gas flow rate (accuracy ± 2% f.s.v., E5-2600/h, manufactured by ASA, Italy). A pump, controlled by a bypass valve, provides water recirculation, and a rotameter (3) measures the liquid flowrate (accuracy ± 1.5% f.s.v., G6-3100/39, manufactured by ASA, Italy): in the present experimental investigation, the bubble column has been tested in the batch ($U_L = 0$ m/s) and in the counter-current ($U_L = -0.0846$ m/s) modes. The value of the liquid velocity has been selected taking into account our previous results and the literature. Indeed, low liquid velocities do not affect the gas holdup (see, for example, refs. Akita and Yoshida, 1973; de Bruijn et al., 1988; Lau et al., 2004; Rollbusch et al., 2015a; Sangnimnuan et al., 1984; Shah et al., 1982; Shawaqfeh, 2003; Voigt and Schügerl, 1979; Yang and Fan, 2003) because, if U_L is low compared with the bubble rise velocities, the acceleration of the bubbles is negligible (Hills, 1976). On the contrary, at higher liquid velocities (as the one selected in the present study), the column operation influences the gas holdup: the co-current mode reduces the gas holdup, and the counter-current mode increases the gas holdup as bubbles are either accelerated or decelerated by liquid motion (Baawain et al., 2007; Besagni et al., 2014; Besagni et al., 2016a; Biń et al., 2001; Jin et al., 2010; Otake et al., 1981). The values of gas density (used to compute U_G) are based upon the operating conditions existing at the column midpoint (computed by using the ideal gas law) (Reilly et al., 1994). The midpoint column pressure has been assumed equal to the column outlet pressure plus one-half the total experimental hydrostatic pressure head. Within this study, gas superficial velocities in the range between 0.004 (± 0.0005) and 0.23

[3] It is worth noting that this concept provides rational basis for the scale—up criterion 1 of Wilkinson et al. (1992).

Table 1
Literature survey.

Ref.	d_c [m]	H_c [m]	H_0 [m]	AR [-]	Sparger type	d_o [mm]	U_G [m/s]	Working fluids
This study	0.24, circular	5.3	0.24 up to 3.6	1 up to 15	Spider	2 up to 4	up to 0.2	Air/Water
Sasaki et al. (2016)	0.2, circular and square	2	0.3 up to 1	1.5 up to 5	Perforated plate	1.4	0.025 - 0.4	Air/Water
Rollbusch et al (2015a)	0.16, circular	1.8	1.8	11.25	Perforated Plate	1	up to 0.1	Nitrogen/Water, aqueous solutions of cumene and acetone
	0.30, circular	2.63	2.63	8.75				
	0.33, circular and under pressure up to 3.6 MPa	3.88	3.88	11.25				
Ruzicka et al. (2001a)	0.14/0.29/0.4, circular	–	0.1 up to 1.2	0.25 up to 8.5	Perforated plate	0.5	up to 0.175	Air/Water
Sarrafi et al. (1999)	0.155, circular	–	1.5/1.8	around 10	Perforated plate	1	up to 0.12	Air/Water
Thorat et al. (1998)	0.385, circular	3.2	0.385 up to 2.695	1 up to 7	Perforated plate	1	up to 0.3	Air/Water, Aqueous solution of electrolytes and Carboxymethyl cellulose
Zahradnı́k et al. (1997)	0.14/0.15/0.29, cicular	2.6	0.25 up to 10	1 up to 29	Perforated plate	0.5/1.6	up to 0.15	Air/Water, Aqueous solution of ethanol, saccharose and electrolytes
Wilkinson et al. (1992)	0.158/0.23, circular	–	1.5/1.2	5 up to 10	Ring	2 up to 7	up to 0.28	Nitrogen/n-Heptane, MEG, water
Reilly et al. (1986)	0.30, circular	5.0	3	10*	Single orifice	25.4		
Schumpe and Grund (1986)	0.30, circular	4.4	–	10*	Ring plate *(perforated plate sparger is not considered here)*	1	up to 0.20	Air/Water
							up to 0.16	Air/Water
Patil et al. (1984)	0.38, sectionalized bubble column		0.684/1.026/1406	1.8/2.7 and 3.7	Perforated plate *(single point sparger is not considered here)*	3.57	up to 0.16	Air/Water, CMC, NAOH and acid dichromate solutions
Akita (1973)	0.152, circular	4	2 up to 3	13.2 up to 19.7	single-hole nozzle	5	0.006 up to 0.42	Various gas/liquid mix
Yoshida and Akita (1965)	0.077/0.152/0.301/0.6, circular	–	0.9 up to 3.5	2.1 up to 22.9	Single-hole nozzle	2.25 up to 40	up to 0.25	Air or pure Oxygen/Sodium sulfite solution

*Estimated from the gas holdup data.

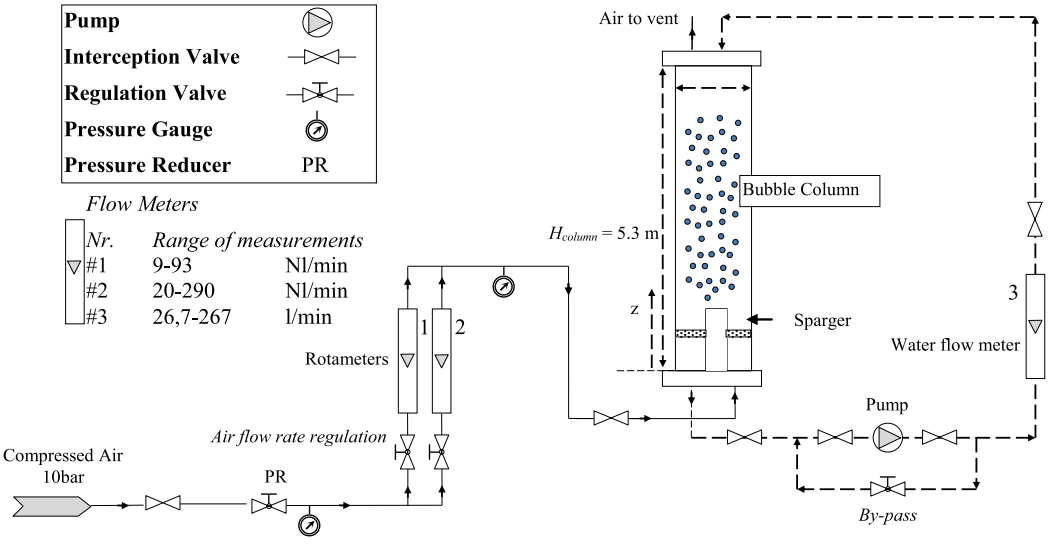

(a) Experimental facility

(b) Spider sparger

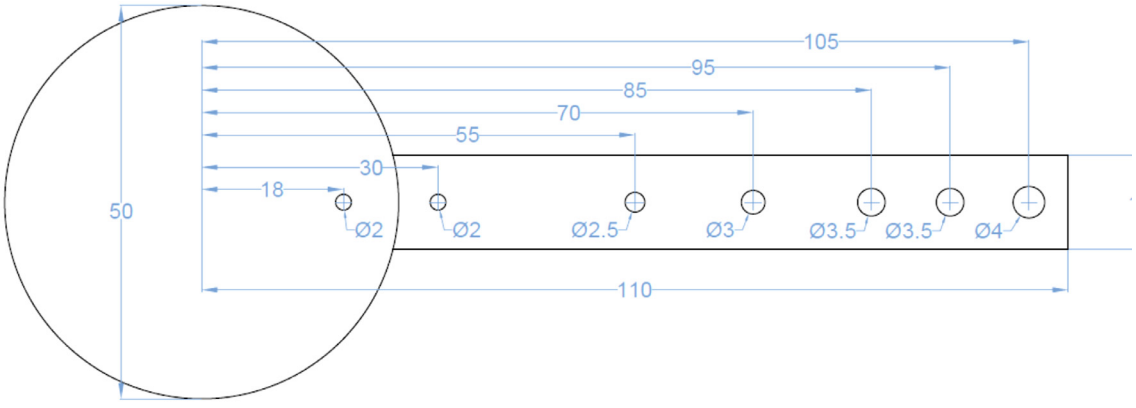

(c) Spider sparger: distribution of the holes on one of the six arms (measurements in mm)

Fig. 1. Experimental setup.

(±0.01) m/s have been considered, where the uncertainties were evaluated at 95% confidence.

The gas distributor, is a spider-gas sparger distributor (Fig. 1b, c) with hole diameters $d_o = 2$–4 mm, which classify this gas sparger as "*coarse*" gas sparger type. The spider gas sparger has six arms made of 0.12 m diameter stainless steel tubes soldered to the center cylinder of the gas sparger. The gas sparger has been installed with the six holes located on the side of each arm facing upward. The holes are distributed as shown in Fig. 1c, with an increasing diameter moving toward the column wall. Additional images and flow visualizations of the spider gas sparger were proposed in refs. Besagni and Inzoli (2016b,c) and Besagni et al. (2016b).

2.1.2. Gas and liquid phases

The gas and liquid temperatures have been checked and maintained constant at room temperature during all the experiments ($T = 295 \pm 1$ K); a survey on the influence of the operating conditions has been proposed by recent reviews (Leonard et al., 2015; Rollbusch et al., 2015b) and is not repeated here. In the following, a discussion concerning liquid and gas phases is given.

Filtered air from laboratory lines has been used as the gaseous phase in all the experiments; the air-cleaning line consists in filters (mechanical and activated carbon) and condensation drying unit, in order to clean the gas phase properly and, thus, to avoid the presence of contaminants in form of (i) solid particles and (ii) organic substances.

The liquid phase has included deionized water and different aqueous solutions of sodium chloride as electrolyte (kitchen quality, NaCl 98.52% in mass). During the experimentation, care has been taken to ensure that the bubble column has been always clean to minimize any contamination that might affect the results (the system has been previously flushed to remove contaminants and to avoid the presence of additional surfactants). The inclusion of NaCl to the liquid phase changes (a) the interfacial bubble properties and (b) the physical properties of the mixture. Both these aspects are discussed in the following.

Effect of Nacl on interfacial bubble properties. To the authors' opinion, to understand the influence of NaCl on bubble column fluid dynamics, the main concept is the bubble coalescence suppression induced by the electrolytes (i.e., see refs. Craig et al., 1993; Deschenes et al., 1998; Firouzi et al., 2015; Keitel and Onken, 1982; Marrucci and Nicodemo, 1967; Weissenborn and Pugh, 1996). In this respect, the transition molar concentration, n_t, is defined as the concentration, n, of the non-coalescent media above which bubble coalescence is drastically reduced. This concentration has been quantitatively evaluated in the pioneering study of Lessard and Zieminski (1971) by studying coalescence on bubble pairs: they have found that n_t is unique for each salt. Later, the concept of transition concentration has been extended to swarm of bubbles by Craig et al. (1993), by considering NaCl aqueous solutions: they have found that n_t does not depend on U_G. These results have been further extended by Nguyen et al. (2012) for different salts in bubble column: they have found that—except for NaI—n_t does not depend on U_G. Therefore, it is reasonable and correct to use the concept of transition concentration to characterize the bubble column fluid dynamics and to relate the "*bubble-scale*" to the "*reactor-scale*" (the importance of the relations between the bubble and the reactor scale has been clearly demonstrated in one of our previous study, ref. Besagni et al., 2016b). In particular, depending on the electrolyte concentration, n, we may define a "*coalescent flow regime*" ($n^* \leq 1$) and a "*non-coalescent flow regime*" ($n^* > 1$), through the dimensionless concentration, n^*—following the formulation of n_t proposed by Prince and Blanch (1990) (which is a modified version of the first formulation of Marrucci (Marrucci and Nicodemo, 1967)):

$$n^* = n/n_t \xrightarrow{\text{(Prince and Blanch, 1990)}} n/\left\{1.18\frac{\mu_L}{\rho_L}\left(\frac{B\sigma}{r_b}\right)^{0.5} R_g T\left(\frac{\partial\sigma}{\partial n}\right)^{-2}\right\} \tag{2}$$

Where B is the retarded Hamaker constant ($B = 1.5 \times 10^{-28}$ J m), R_g is the gas constant, T is the temperature of the system, r_b is the bubble radius, and σ and $\partial\sigma/\partial$n are the surface tension and the surface tension gradient with electrolyte concentration, respectively. In the case of NaCl, different values of n_t have been reported in the literature, based on different measurement techniques (i.e. adjacent capillaries, light intensity in bubble column, size distributions in bubble column and micro-interferometry, as reviewed by Firouzi et al., 2015) and, in this study, we selected $n_t = 0.145$ mol/l, following the study of Zahradník et al. (1999). Notice that $n_t = 0.145$ mol/l is in agreement with the prediction of Eq. (2). This value has been obtained by considering adjacent capillaries and is, therefore, a property related to the "*bubble-scale*" ; the reader should refer to Besagni and Inzoli (2015, 2016c) for the discussion concerning the effect of the electrolytes on the "*reactor-scale*" (i.e., gas holdup and flow regime transitions). It is worth noting that Ribeiro and Mewes (2007), have obtained similar gas holdup curves regardless of the electrolyte for given dimensionless concentration, n^*: therefore, Eq. (2) is a promising modelling parameter to account for the chemical nature of electrolytes and would be useful to extend our experimental results (Section 4.3) to other systems. Future researchers might use Eq. (2) to obtain n_t for a generic electrolyte and, by using our experimental data, they might easily interpret our results by using different definition.

Effect of Nacl on the physical properties. When including NaCl in the liquid phase, not only the properties at the interface change, but also the physical properties of the binary mixture. In this respect, the properties of the binary mixture were estimated based on the information provided in ref. Hai-Lang and Shi-Jun (1996) and are summarized in Fig. 2, for the sake of clarity. It is worth noting that salt-quality NaCl has almost identical physical properties of pure NaCl, within the error of determination, as deeply discussed by Orvalho et al. (2009). In the discussion of the results we demonstrate that the fluid dynamics in bubble columns can not be entirely explained and modelled by using the bulk physical properties of the liquid phase (i.e., the surface tension, density and liquid phase viscosity). This point was also discussed in the remarkable study by Shah et al. (1985) and can be concluded also based on our previous works concerning the influence of organic active compounds (Besagni et al., 2016b) and viscous liquid phase (Besagni et al., 2017).

2.2. Gas holdup measurements

The gas holdup (ε_G), which is considered a global fluid dynamic parameter (at the "*reactor-scale*"), is a dimensionless parameter defined as the volume of the gas phase divided by the total volume. Measurements of the bed expansion allowed the evaluation of ε_G: the procedure involves measuring the location (height) of the liquid free surface when air flows in the column. The gas holdup is then obtained using Eq. (3):

$$\varepsilon_G = \frac{V_G}{V_{L+G}} \xrightarrow{\text{Constant cross-section-area}} \frac{(H_D - H_0)}{H_D} \tag{3}$$

Where V_G is the volume of the dispersed phase, V_{L+G} is the total volume, H_D is the height of the free-surface after aeration and H_0 is the height of the free-surface before aeration. H_0 is varied in order to study the influence of different AR (in the range $1 \leq AR \leq 15$). It is worth noting that height measurements are performed from gas sparger opening as reference location. The com-

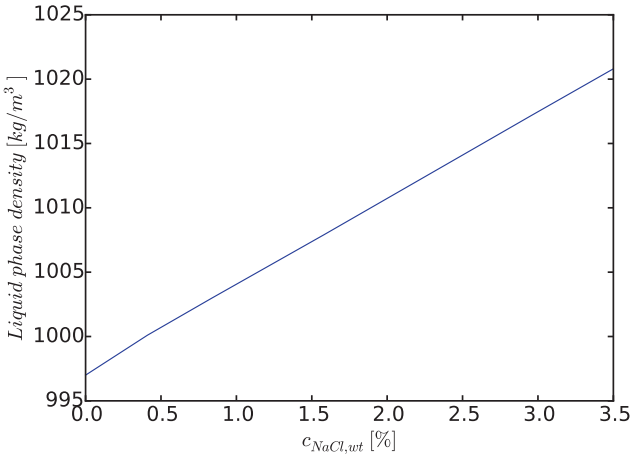

(a) Liquid phase density of the water-NaCl mixture

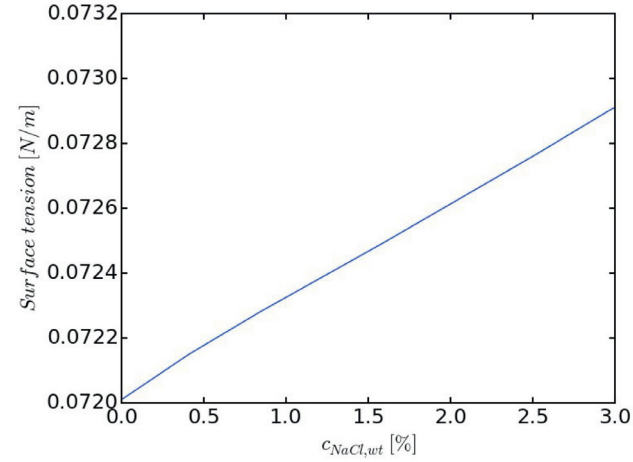

(b) Surface tension of the water-NaCl mixture

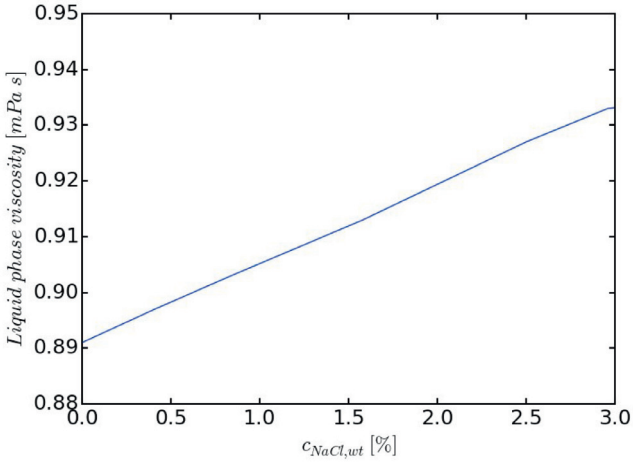

(c) Liquid phase viscosity of the water-NaCl mixture

Fig. 2. Physical properties of the water-NaCl binary mixture.

plete uncertainty analysis in the estimation of the gas holdup is proposed in Appendix A.

The gas holdup curve (the relationship between $\varepsilon_G - U_G$) provides information of the global bubble column fluid dynamics and can be used to study the flow regime transitions (as described in Section 2.3). Indeed, applying the mass conservation to the gas phase, the gas holdup is computed as:

$$\varepsilon_G = U_G/U_{swarm} \rightarrow U_{swarm} = U_G/\varepsilon_G \propto t_G \tag{4}$$

Where U_{Swarms} is the mean rise velocity of the gas phase (it can be computed by the experimental measurements obtained through Eq. (4)) and t_G is the mean residence time of the gas phase. U_{Swarms} is strictly related to the coupling between the phases and the main parameters (i.e., bubble sizes, rise velocities, …) and, thus, to the mean residence time of the gas phase, t_G (Orvalho et al., 2009; Ruzicka et al., 2008).

2.3. Analysis of the flow regime transitions

In this section, the flow regimes in a large-diameter bubble column are described and the methods (by the interpretation of the $\varepsilon_G - U_G$ curve) to detect the flow regime transition points are presented. Although the flow regime transitions do not occur instantaneously, the definition of an approximate transition point is helpful to understand and model the hydrodynamic behavior of bubble columns, as deeply discussed by Krishna et al. (1991), and to develop gas holdup correlations, as discussed in Section 4.

2.3.1. Flow regimes in large-diameter bubble columns

The global and the local fluid dynamic parameters of a bubble column are related to the prevailing flow regimes. In the literature, different definitions of flow regimes have been proposed and there is not agreement: for example, many definitions of the homogeneous flow regime were proposed, as reviewed by Besagni et al. (2016b, 2017). The goal of this section is to clearly present and describe the flow regimes, and extend the discussion proposed in our previous papers. Generally, the fluid dynamics in bubble columns is determined by the momentum exchange between the liquid and the gas phases. In this respect, the fluid dynamics in a bubble column is governed by the same mechanisms as the other vertical pipe flows (i.e., momentum exchange, …). In vertical pipe flows, with non-foaming systems (see ref. Shah et al., 1985), four main types of flow patterns can be observed when increasing the gas flow rate (and, thus, the superficial gas velocity, U_G), at fixed system design and phase properties: (a) the homogeneous flow regime, (b) the heterogeneous flow regime; (c) the slug flow regime; (d) the annular flow regime. In industrial applications, large-diameter (defined by Eq. (1)) and large-scale bubble columns are used: in this situation, two main flow regimes (and the transition flow regime in-between) are observed (see, for example, the well-known flow maps in ref. Shah et al., 1982):

(i) the homogeneous flow regime;
(ii) the transition flow regime;
(iii) the heterogeneous flow regime.

Indeed, in practical applications, the annular flow regime is not observed because of the very high gas velocities requested (see the method in ref. Pagan et al., 2017). Conversely, the slug flow regime is not observed because of the fluid dynamics phenomena and, in particular, because of the Rayleigh–Taylor instabilities (Kitscha and Kocamustafaogullari, 1989). The quantification of the Rayleigh–Taylor instabilities at the "*reactor-scale*" is quantified through Eq. (1). Therefore, two main transitions exist in large-diameter bubble columns:

(i) the transition between the homogeneous and the transition flow regimes ($\varepsilon_{G,trans,I}$, $U_{G,trans,I}$);
(ii) the transition between the transition and the heterogeneous flow regimes ($\varepsilon_{G,trans,II}$, $U_{G,trans,II}$).

The main features of these flow regimes as discussed in the following.

Homogeneous flow regime. The homogeneous flow regime—generally associated with small gas superficial velocities—is referred as the flow regime where "*non-coalescence-induced*" bubbles exist (as detected by the gas disengagement technique (Besagni and Inzoli, 2016b) and visualized by Sasaki et al., 2016). The homogeneous flow regime can be further distinguished into "*pure-homogeneous*" (or "*mono-dispersed homogeneous*") flow regime and "*pseudo-homogeneous*" (or "*poly-dispersed homogeneous*" or "*gas maldistribution*") flow regime: the former is characterized by a mono-dispersed BSD (as the one observed by Mudde et al. (2009), by using a "*fine*" gas sparger), whereas the latter is characterized by a poly-dispersed BSD (if large bubbles are aerated (Besagni and Inzoli, 2016a, b), by using a "*coarse*" gas sparger). We define the mono-dispersed and poly-dispersed BSDs accordingly with the change of sign in the lift force coefficient (Besagni and Inzoli, 2016b; Besagni et al., 2016b, 2017; Lucas et al., 2015; Zahradník et al., 1997; Ziegenhein et al., 2015).

Transition flow regime. The transition from the homogeneous flow regime to the heterogeneous flow regime is a gradual process, in which a transition flow regime occurs. This flow regime is characterized by large flow macro-structures with large eddies and a widened bubble size distribution (BSD) due to the onset of bubble coalescence; it is identified by the appearance of "*coalescence-induced*" bubbles, as defined and observed by Besagni et al. (2016b), and visualized by Sasaki et al. Sasaki et al. (2016, 2017) when "*coalescing*" solutions are employed. Conversely, if "*non-coalescing*" solutions are employed, the transition flow regime is identified by the appearance of "*clusters of bubbles*", as defined in refs. Takagi and Matsumoto (2011) and Takagi et al. (2008) and observed by Besagni and Inzoli (2016b) and Besagni et al. (2016b). Besagni et al. (2017) demonstrated that "*coalescence-induced*" bubbles (and, thus, the destabilization of the homogeneous flow regime) are caused by the lift force pushing the larger bubbles toward the center of the bubble column (see Section 3.4 in Besagni et al., 2017). Similarly, Takagi et al. (Takagi and Matsumoto, 2011; Takagi et al., 2008) discussed how the "*clusters of bubbles*" are formed because of the lift force acting on a mono-dispersed BSD. Beinhauer (1971) found that the first "*coalescence induced*" bubble appeared at about $U_G = 0.02$ m/s and, increasing the gas superficial velocities, both "*non-coalescence-induced*" and "*coalescence induced*" increase till the *non-coalescence-induced*" bubbles reached a maximum and, then, decrease toward a constant value. Conversely, Schumpe and Grund (1986), Krishna and co-workers (Krishna et al., 2000a; Krishna et al., 2000b) and Besagni and Inzoli (2016b) reported that the *non-coalescence-induced*" bubbles increase till the flow regime transition point and, then, only "*coalescence induced*" bubbles increase. The difference is probably caused by the different gas sparger design ("*fine-gas sparger*" and "*coarse-gas sparger*").

Heterogeneous flow regime. At high gas superficial velocities, a fully heterogeneous flow regime is reached (Sharaf et al., 2015); it is associated with high coalescence and breakage rates and a wide variety of bubble sizes. A recent, and interesting, review on the mechanisms governing the flow regime transition towards the heterogeneous flow regime has been proposed by Montoya et al. (2016).

The transitions between the different flow regimes depend on the operation mode, design parameters and working fluids of the bubble column. For example, considering the effect of the gas sparger, a "*fine*" gas sparger that produces mainly very small bubbles the homogeneous flow regime is stabilized (Mudde et al., 2009), whereas the mono-dispersed homogeneous flow regime may not exist if large bubbles are aerated (Besagni and Inzoli, 2016a, b) up to a "*pure heterogeneous flow regime*" from the beginning (Ruzicka et al., 2001b). Concerning the influence of the liquid phase properties, ethanol and electrolyte stabilize the homogeneous flow regime and suppress the "coalescence-induced" bubbles (Besagni and Inzoli, 2015; Besagni et al., 2016b) and viscous solutions exhibited a "*dual effect*" depending on the nature of the prevailing BSD.

In the present bubble column, the "*mono-dispersed homogeneous*" does not exist (as observed in our previous study, Besagni and Inzoli, 2016b) and the existing flow regimes are: (i) "*pseudo-homogeneous flow regime*", (ii) transition flow regime and (iii) heterogeneous flow regime.

2.3.2. First flow regime transition point

In our previous papers we showed how the swarm velocity and the drift-flux/Wallis plot methods have been able to identify the first flow regime transition point (Besagni and Inzoli, 2016b). In particular, the first flow regime transition point (in terms of the transition gas velocity and transition gas holdup) is computed as the average of the values obtained by the two methods:

$$U_{G,trans,I} = \frac{U_{G,trans,swarm} + U_{G,trans,Wallis}}{2} \tag{5}$$

$$\varepsilon_{G,trans,I} = \frac{\varepsilon_{G,trans,swarm} + \varepsilon_{G,trans,Wallis}}{2} \tag{6}$$

The details concerning the two methods are provided below.

2.3.2.1. Swarm velocity method. The swarm velocity method has been developed by Zuber and Findlay (1965) and is based on the swarm velocity, U_{swarm}, (Eq. (4)). The swarm velocity is plotted against the gas superficial velocity: U_{swarm} is almost constant in the homogeneous flow regime (or, in some cases, it can be slightly decreasing), but it starts to increase as the system enters the transition flow regime at a transition superficial velocity, $U_{G,trans,I}$. The appearance of the first "*coalescence-induced*" bubble is responsible for this sudden increase in the swarm velocity and is an indication of the flow regime transition. In this study, the quantitative evaluation of $U_{G,trans,swarm}$ has been determined by the intersection between the trends of U_{swarm} in the two flow regimes.

Thus, U_{swarm} has been taken as constant in the homogeneous flow regime (Eq. (7)):

$$U_{swarm,\text{homogeneous}} = \text{constant} \tag{7}$$

Whereas, in the transition flow regime it has been determined by a least squares fitting of the following function:

$$U_{swarm,\text{transition}} = S_1 (U_G)^{S_2} + S_3 \tag{8}$$

Where S_1, S_2 and S_3 are fitting parameters.

The transition point ($U_{G,trans,swarm}$, $\varepsilon_{G,trans,swarm}$) is thus evaluated by solving the following Eq. (9):

$$U_{swarm,\text{homogeneous}} = U_{swarm,\text{transition}} \tag{9}$$

2.3.2.2. Drift-flux/Wallis plot method. The drift-flux method has been proposed by Wallis (1969) and has been widely applied in the literature. This method is based on the drift-flux, which represents the gas flux through a surface moving with the speed of the two-phase mixture and is experimentally obtained as follows:

$$J_T = U_G(1 - \varepsilon_G) \pm U_L \varepsilon_G \tag{10}$$

The complete derivation of Eq. (10) has been described and detailed by Besagni and Inzoli (2016c) and is further discussed in Appendix B, for the sake of clarity within this research. In Eq. (10), the sign on the right side of the equations depends on the operation mode of the bubble column: (a) the co-current mode (+) or (b) the counter-current mode (-). In this work, only the batch mode and the counter-current mode were considered.

Theoretically, the drift-flux is written in terms of the bubble swarm velocity, whose dependence upon ε_G varies with the prevailing flow regime:

$$J_E = U_b(1-\varepsilon_G) \tag{11}$$

The idea in this method is to employ a model for U_b that is valid for the homogeneous flow regime, plot J_E and J_T in the same graph as a function of ε_G. Since the formulation is valid for the homogeneous flow regime, by plotting J_E and J_T against the gas holdup on the same graph, it is possible to determine the transition point from one flow regime to the other one as the point where the curve of J_E deviates from the curve of J_T. Thus, the transition point is defined when:

$$J_T \neq J_E \tag{12}$$

The evaluation of U_b in Eq. (11) is a matter of discussion in the literature and different models have been proposed and applied. In this study, the approach of Krishna et al. (2000b) has been followed, which is based on the empirical model of Richardson and Zaki (1997):

$$U_b = u_\infty \varepsilon_G (1-\varepsilon_G)^{o-1} \tag{13}$$

Where o is fluid-dependent and u_∞ is the terminal velocity of an isolated bubble. These values should be fitted with the aid of the experimental data in the determination of the transition point.

Combining Eqs. (11) and (13), the following equation is derived:

$$J_E = u_\infty \varepsilon_G (1-\varepsilon_G)^{o} \tag{14}$$

2.3.3. Second flow regime transition point

The second flow regime transition is estimated following the proposal of Sharaf et al. (2015), which relies on the drift-flux method for multiphase systems proposed (Zuber and Findlay, 1965). Within this approach, ε_G is computed as follows (the reader should refer to the paper of Zuber and Findlay for the complete derivation of this method):

$$\varepsilon_{G,Zuber-Finley} = \frac{U_G/(U_G+U_L)}{C_0 + [u_d/(U_G+U_L)]} \tag{15}$$

Where C_0 is the distribution parameter (to account for radial profile effects in the cross-section of the column) and u_d is the weighted mean drift velocity. These parameters can be computed by using either a local or a global approach: (i) the local approach relies on local flow (liquid phase velocity and local void fractions) measurements, whereas (ii) the global approach relies on fitting the gas holdup curve. In the batch mode ($U_L = 0$ m/s), Eq. (15) reads as:

$$\varepsilon_{G,Zuber-Finley} = \frac{U_G/(U_G+U_L)}{C_0 + [u_d/(U_G+U_L)]} \xrightarrow{U_L=0} \frac{1}{C_0 + [u_d/U_G]} = \frac{U_G}{U_G C_0 + u_d} \tag{16}$$

In this study C_0 and u_d have been determined by a least squares fitting with the experimental data (the global approach) at $U_G > 0.15$, as the second flow regime transition is expected about 0.1 m/s accordingly to Nedeltchev (2015) and Sharaf et al. (2015).

The transition point ($\varepsilon_{G,trans,II}$, $U_{G,trans,II}$) is, thus, evaluated by solving the following Eq. (17):

$$\varepsilon_{G,Experimental} \neq \varepsilon_{G,Zuber-Finley} \tag{17}$$

3. The experimental results

Herein the experimental results (the gas holdup and flow regime transition points) have been presented. At first, the effect of *AR* (on the gas holdup and flow regime transitions) in coalescing systems (air-water) in the batch mode and in the counter-current mode has been discussed. At second, the influence of *AR* (on the gas holdup and flow regime transitions) in non-coalescing systems (air-water-NaCl) has been discussed. These experimental data have been used to assess novel gas holdup correlations (Section 4).

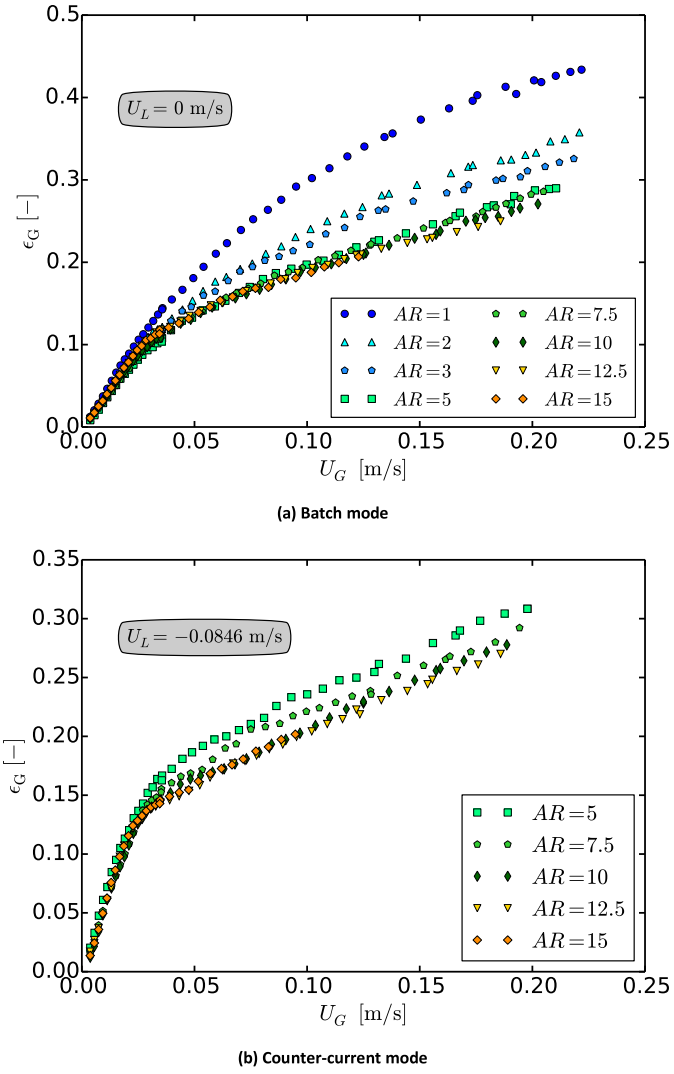

Fig. 3. Gas holdup measurements: air-water system.

3.1. The effect of aspect ratio in coalescing (air-water) systems: batch mode

3.1.1. Gas holdup

Fig. 3a displays the gas holdup curves in the batch mode for the different *ARs* (in the range $1 \leq AR \leq 15$). All the gas holdup curves are similar in shape and the relation between ε_G and U_G can be interpreted by the proportionality:

$$\varepsilon_G \sim U_G^{\beta} \tag{18}$$

Where the exponent β depends on the bubble column fluid dynamics (i.e., the flow regimes, the coupling between the phases, ...). At low gas superficial velocities—in the pseudo-homogeneous flow regime—the relationship between ε_G and U_G is linear ($\beta > 1$), followed by a change in tendency, caused by the appearance of "*coalescence-induced*" bubbles, at the first flow regime transition. After the flow regime transition, the appearance of "*coalescence-induced*" bubbles increases the average rise velocity of the dis-

persed phase and reduces the mean gas residence time in the bubble column (Besagni and Inzoli, 2016b; Yang et al., 2010), thus reducing the gas holdup versus gas velocity slope ($\beta < 1$). The values of β in Eq. (18) have been already discussed by De Guido et al. (2016) and are in agreement with the theoretical expectations: applying the mass conservation to the gas phase, the gas holdup is computed as $\varepsilon_G = U_G/u_{G,}$ where u_G is the mean rise velocity of the gas phase. If the bubbles would travel at their terminal velocity, the gas holdup would increase linearly with the gas flow rate; however, the coupling between the phases causes deviations from linearity (see, refs. Besagni and Inzoli, 2016c; Ruzicka et al., 2003): (i) in the homogeneous flow regime, the hindrance reduces the bubble velocity, thus increasing ε_G; (ii) in the transition/heterogeneous flow regime the "*coalescence-induced*" bubbles and the enhanced circulations cause ε_G to decrease less than proportionally to U_G. The shape of the gas holdup curves is the one typically found for similar gas sparger geometries; indeed, the shape of the gas holdup curve is mainly related the gas sparger design (if large-diameter columns are considered, see, for example, ref. Sharaf et al., 2015): (a) "*fine gas spargers*" ($d_o < 1$ mm; see, for example, ref. Mudde et al., 2009) produce mono-dispersed BSBs, leading to the hindrance effect, which is physically manifested by the peak on the gas holdup curve (please notice that the reversed S-shaped curve can be interpreted on the basis of the Ledinegg instability); (b) "*coarse gas spargers*" ($d_o > 1$–2 mm, as suggested by the scale-up criteria of Wilkinson et al. (1992), as the one employed in this study, lead to monotonic increasing gas holdup curves, which is described by the proportionality, Eq. (18).

The gas holdup decreases continuously while increasing *AR* up to the critical aspect ratio, $AR_{Cr} = 5$. Above AR_{Cr}, there is no remarkable difference in the gas holdup curves: our experimental observations confirm the existence of a critical aspect ratio above which the gas holdup does not depend anymore from *AR*. The value of the critical aspect ratio, $AR_{Cr} = 5$, is in agreement with the scale-up criteria of Wilkinson et al. (1992) and the experimental observation of other authors (i.e., refs. Thorat et al., 1998; Zahradnik et al., 1997). Moreover, the decrease in the gas holdup while increasing *AR* is in agreement with the experimental observations of different authors (Sasaki et al., 2016; Thorat et al., 1998; Zahradnik et al., 1997) and is probably be caused by the coalescence phenomena. In systems where the bubble sizes are not at their maximum equilibrium size, ε_G would decrease while increasing H_0: the higher the column, the longer the time available for bubble coalescence. This concept is further explained when considering the influence of the liquid velocity (Section 3.2) and non-coalescing liquid phases (Section 3.3).

We have compared our results with a set of experimental studies with similar column diameters and gas sparger designs: Fig. 4 displays the gas holdup data considered and Table 1 summarizes the details of the studies considered (Akita and Yoshida, 1973; Patil et al., 1984; Reilly et al., 1986; Rollbusch et al., 2015a; Ruzicka et al., 2001a; Sasaki et al., 2016; Sasaki et al., 2017; Schumpe and Grund, 1986; Thorat et al., 1998; Wilkinson et al., 1992; Yoshida and Akita, 1965). A further comparison with the literature is provided in our previous paper (Besagni and Inzoli, 2016b). When gas holdup data are compared between different configurations—at the same operating conditions for given gas and liquid phases—the following design parameters must be considered (Rollbusch et al., 2015a), following the criteria of Wilkinson et al. (1992): (i) d_c, (ii) d_o and (iii) *AR*. All the studies considered in Fig. 3 are large-diameter ($d_c \gtrsim 0.15$ m) and, thus, the wall effects can be neglected. The shape of the gas holdup curves can be easily interpreted based on considerations concerning the gas sparger opening, d_o. As previously stated (Section 2.3.1), "*coarse*" gas spargers ($d_o \gtrsim 1$ mm) ensure a "*poly-dispersed*" homogeneous flow regime (Besagni and Inzoli, 2016a, b) or a pure-heterogeneous flow regime (Ruzicka et al., 2001b); on the other hand, "*fine*" gas spargers ($d_o \gtrsim$ $?> 0.5 - 1 mm) ensure a "*mono-dispersed*" homogeneous flow regime (Mudde et al., 2009). Taking into account this consideration, the shapes of the gas holdup curves obtained by Ruzicka et al. (2001a) are not surprisingly; they have used a "*fine*" gas sparger ($d_o = 0.5$ mm), which leads to a "*mono-dispersed*" homogeneous flow regime: the real uniformity leads to the hindrance effect that physically manifests by the peak on the gas holdup graph (Ruzicka et al., 2001a; Zahradnik et al., 1997). Thorat et al. (1998) and Schumpe and Grund (1986) have used a sieve plate gas sparger ($d_o = 1$ mm) and a ring plate gas sparger ($d_o = 1$ mm), respectively: these gas spargers lead to a gas holdup curve intermediate between a peaked curve and a monotonically increasing curve. On the contrary, Sasaki et al. (2016, 2017), Patil et al. (1984), Yoshida and Akita (1965) and Wilkinson et al. (1992) have used "*coarse*" and "*very-coarse*" gas spargers and, therefore, the gas holdup curve is monotonically increasing, similarly to the shape of our experimental results (Fig. 3a). Rollbusch et al. (2015a) have obtained a monotonically increasing gas holdup curve using a perforated plate gas sparger with $d_o = 1$ mm, however, it is worth noting that Rollbusch et al. (2015a) used Nitrogen as gas phase. As far as *AR* is concerned, Sasaki et al. (2016, 2017), Ruzicka et al. (2001a) and Thorat et al. (1998) have found that an increase in H_0 decreases the gas holdup. Patil et al. (1984) have observed a very low effect of *AR* on the gas holdup, which can be explained by the "*very-coarse*" gas sparger used, which causes a pure-heterogeneous flow regime. It is well known that the effect of the bubble column design is lower in the heterogeneous flow regime. Finally, Sasaki et al. (2017) further developed their previous work (Sasaki et al., 2016) and studied large-diameter bubble columns at low-intermediate *AR* (d_C in the range of 0.16 – 0.3 m - AR up to 6.5, Fig. 4a) and very-large-diameter bubble column at low *AR* ($d_C = 2$ m - AR up to 2, Fig. 4b); they concluded that the gas holdup is independent of the column design in large-diameter and high *AR* bubble column. It seems that, in very-large-diameter bubble columns, the effect of the initial liquid level is lower. In particular, they stated that the effects of the bubble column design parameters become negligible for $d_C \geqslant 200$ mm and $H_0 \gtrsim 2200$ mm, regardless of AR. The conclusion of this study is quite interesting and, at present, this is the only study with tends to disagree on the concept of *AR* as scale-up criterion; unfortunately, no data were available for very-large-diameter bubble columns at high *AR*.

3.1.2. Flow regime transitions

The first and the second flow regime transitions (as defined in Section 2.3.1) have been analyzed by applying the methods presented in Sections 2.3.2 and 2.3.3. Fig. 5a and c display the first and the second transition points and show the boundaries of the homogeneous, the transition and the heterogeneous flow regimes. In particular Fig. 5a displays the influence of *AR* on the transition gas velocities ($U_{G,trans,I}$ and $U_{G,trans,II}$) and Fig. 5c displays the influence of *AR* on the transition gas holdups ($\varepsilon_{G,trans,I}$ and $\varepsilon_{G,trans,II}$).

The homogeneous flow regime is destabilized (decrease in $U_{G,trans,I}$ and $\varepsilon_{G,trans,I}$) while increasing *AR*, up to the critical aspect ratio, $AR_{Cr} = 5$, in agreement with some of the previous studies (Ruzicka et al., 2001a; Sasaki et al., 2016; Zahradnik et al., 1997). Indeed, in short bubble columns (low *AR*) three phenomena tend to destabilize the homogeneous flow regime: (i) the coalescence phenomena are more important (as described in Section 3.1.1), (ii) the liquid circulation patterns are not fully developed and (iii) the end-effects (i.e., the gas sparger and top-column) are more important (Xue et al., 2008). A dual effect has been observed for second flow regime transition: the transition flow regime is stabilized (increase in $U_{G,trans,II}$ and $\varepsilon_{G,trans,II}$) up to $AR = 8$ and it is destabilized (decrease in $U_{G,trans,II}$ and $\varepsilon_{G,trans,II}$) for higher *AR*. The range of values for $U_{G,trans,II}$ is in agreement with the ones presented in some

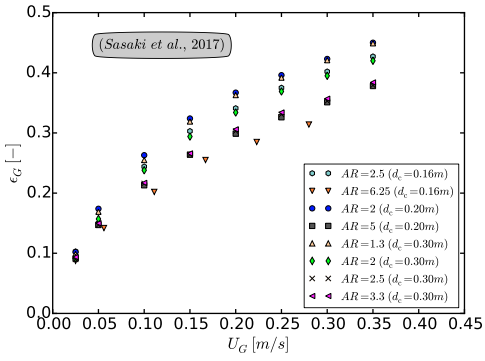

(a) (Sasaki et al., 2017) – d_c < 2 m

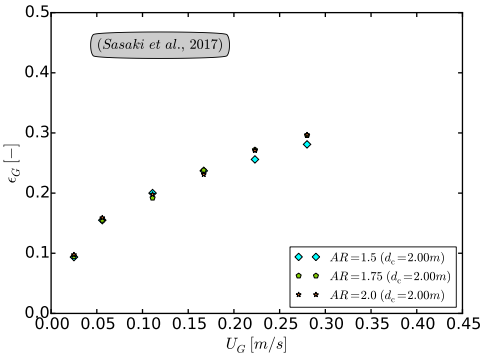

(b) (Sasaki et al., 2017) – d_c = 2 m

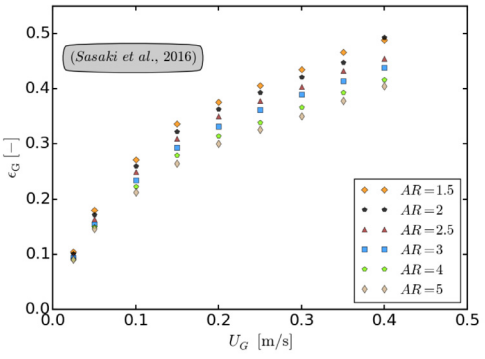

(c) (Sasaki et al., 2016)

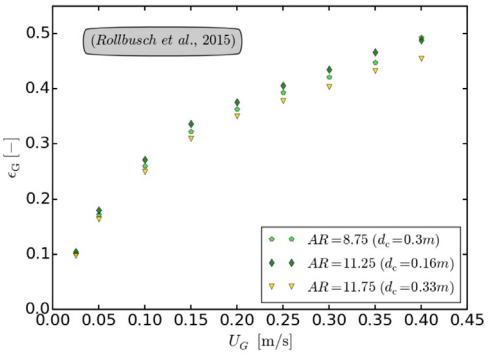

(d) (Rollbusch et al., 2015)

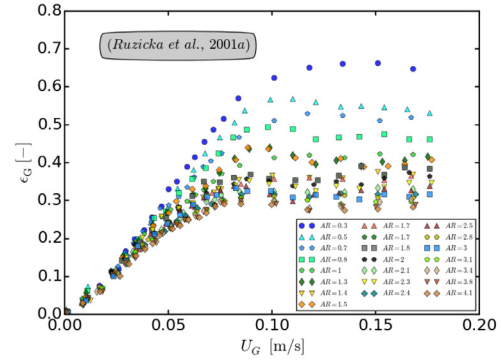

(e) (Ruzicka et al. 2001a)

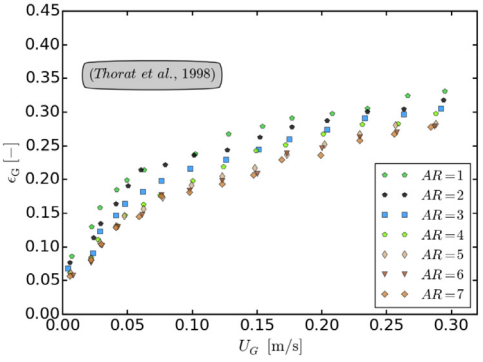

(f) (Thorat et al., 1998)

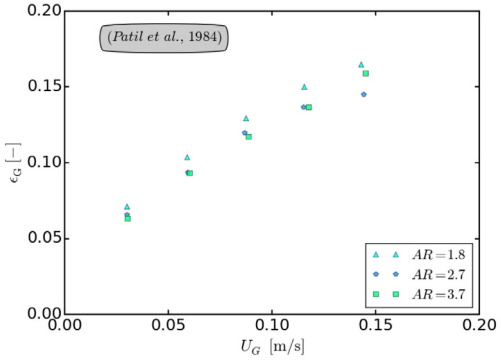

(g) (Patil et al., 1984)

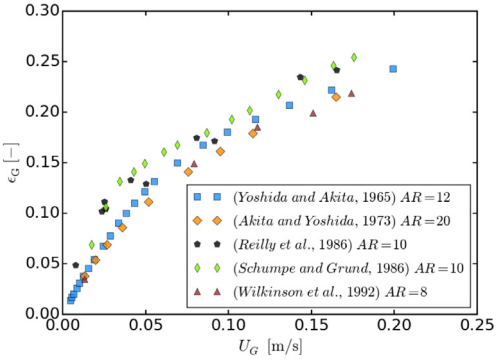

(h) Other studies

Fig. 4. Gas holdup measurements: data from the literature.

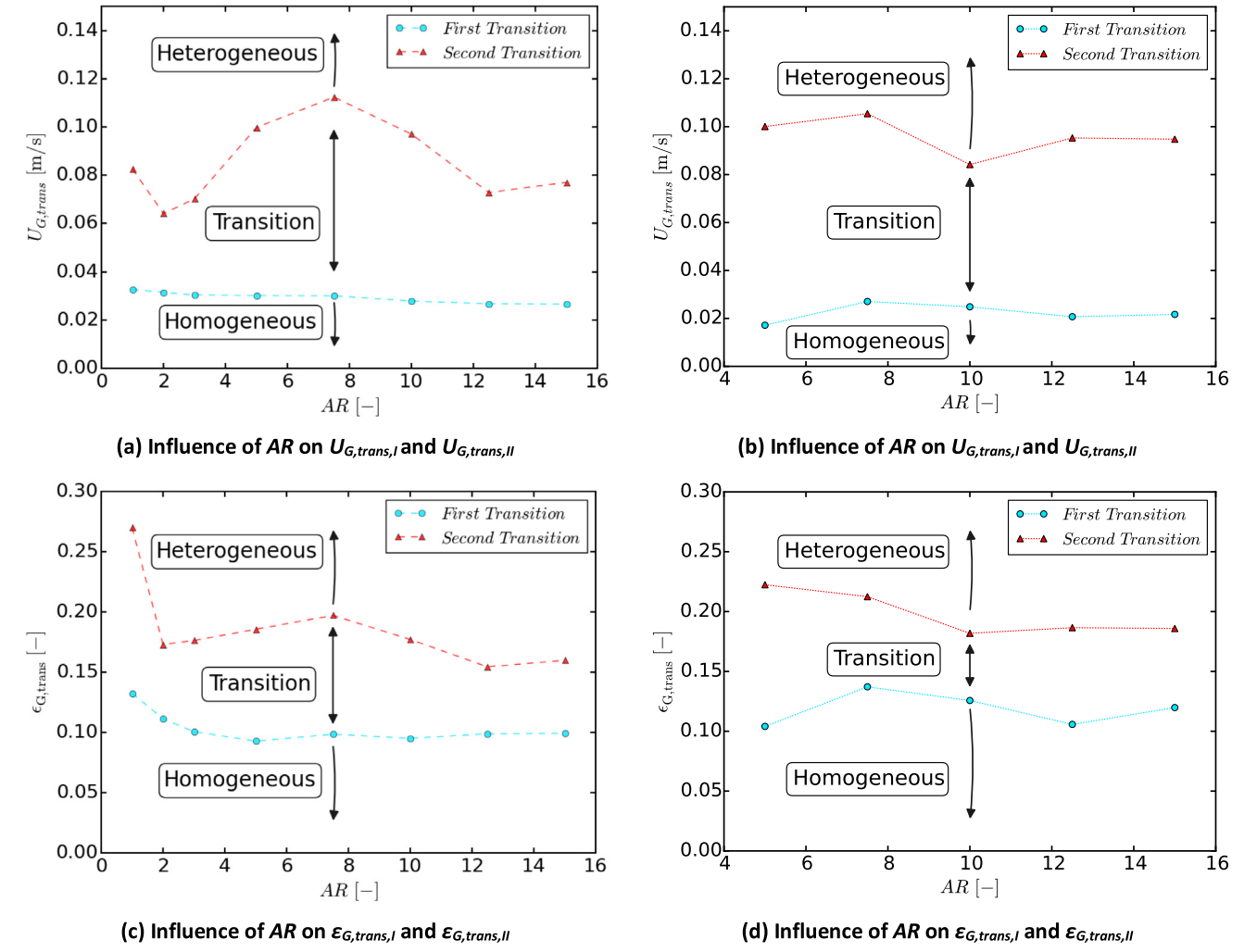

Fig. 5. Flow regime transitions: air-water system.

of the previous studies dealing with the second flow regime transition (Nedeltchev, 2015; Sharaf et al., 2015) (please notice that there is a lack of study concerning the second flow regime transition). It is worth noting that the second flow regime transition points are more scattered, because of the complex phenomena involving the second transition (Montoya et al., 2016).

There is a lack of studies concerning the influence of *AR* on the first and (mainly, as already stated) the second flow regime transitions. In order to fill this gap, we have interpreted the $\varepsilon_G - U_G$ curves taken from the literature (Fig. 3) by the methods presented in the Sections 2.3 obtaining quantitative data on the first and the second flow regime transitions. It should be noticed that, by using this procedure, the flow regime transition points obtained are coherent, as they rely on the same definition. Only the studies having monotonically increasing gas holdup curves have been considered (as described in Section 3.1.1). The results are displayed in Fig. 6; in particular, Fig. 6a ($U_{G,trans,I}$) and Fig. 6c ($\varepsilon_{G,trans,I}$) display the first flow regime transition points and Fig. 6b ($U_{G,trans,II}$) and Fig. 6d ($\varepsilon_{G,trans,II}$) display the second flow regime transition points. From these results four considerations are drawn: (i) the second flow regime transitions are more scattered than the first flow regime transitions (as previously observed); (ii) a relation between the transition points and *AR* clearly exist: the homogeneous flow regime is destabilized while increasing *AR*, up to the critical aspect ratio; (iii) the value of AR_{Cr} for the gas holdup is observed also for the flow regime transitions: above AR_{Cr}, the flow regime transitions (in particular, the first transition) do not change anymore; (iv) the flow regime transition points (in particular, the first transition) between the different studies are in agreements, which is explained by the bubble columns similar in design (i.e., only the studies having monotonically increasing gas holdup curves have been considered). It is worth noting that, owing to the "*large*" gas sparger openings considered, the flow regime transitions occur earlier compared with other literature studies (as reviewed by Besagni and Inzoli, 2016b). This is because, in the batch mode, the larger bubbles generated at the gas sparger (having a negative lift coefficient, see refs. Lucas et al., 2005; Tomiyama et al., 2002), tend to migrate toward the center of the column, thus promoting the appearance of the "*coalescence-induced*" bubbles and, subsequently, the flow regime transition. On the contrary, the small bubbles, having positive lift coefficient, stabilize the homogeneous flow regime.

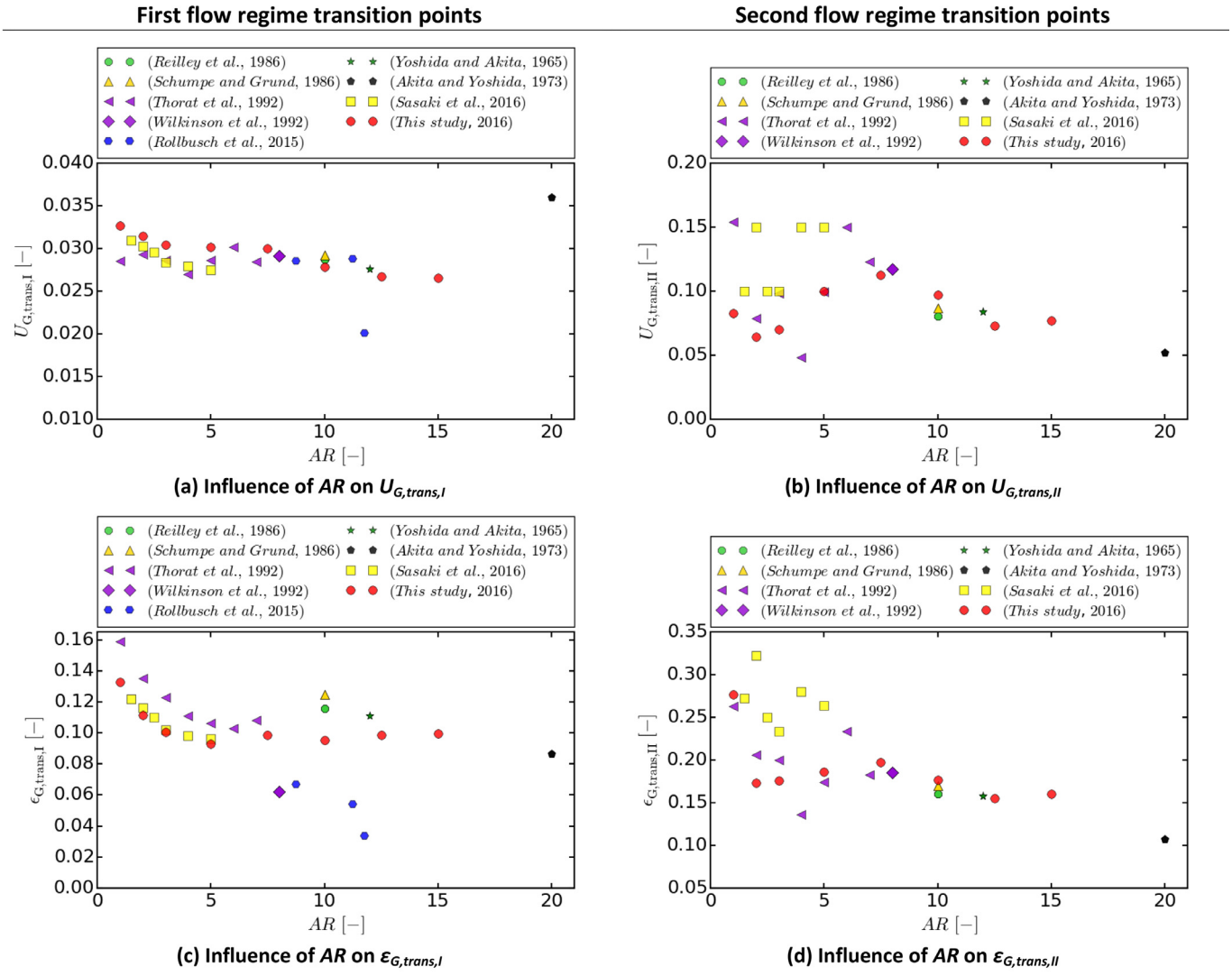

Fig. 6. Flow regime transitions: comparison against data from the literature (air-water system).

3.2. The effect of aspect ratio in coalescing (air-water) systems: counter-current mode

3.2.1. Gas holdup

Fig. 3b displays the gas holdup curves in the counter-current mode ($U_L = -0.0846$ m/s) for the different *ARs* (in the range $5 \leq AR \leq 15$). Compared with the batch mode, upon increasing the liquid flowrate, a faster increase in the gas holdup has been observed at low U_G, and the first transition point moves toward lower gas superficial velocities. This change is explained by the effect of the liquid flow, which slows down the rise of the bubbles, leading to higher gas holdup: the reader should refer to our previous papers (Besagni and Inzoli, 2016b, c) for a complete discussion concerning the influence of the liquid velocity on bubble column hydrodynamics (global and local flow properties). The influence of U_L on the gas holdup is probably caused by the comparable order of magnitude of the liquid and gas velocities. Actually, Hills (1976) mentioned that if U_L is low compared with the bubble rise velocities (represented in terms of U_{swarm} (Rollbusch et al., 2015a)), no impact of U_L on ε_G is expected because the acceleration of the bubbles is negligible and vice-versa. The influence of U_L on the gas holdup is also in agreement with the findings of Otake et al. (1981), Baawain et al. (2007), Biń et al. (2001) and Jin et al. (2010), as described in our previous papers as well. The gas holdup decreases continuously while increasing *AR* up to the critical aspect ratio, $AR_{Cr} = 10$. Above AR_{Cr}, there is no remarkable difference in the gas holdup curves. This observation suggests that the value of AR_{Cr} depends on the operation modes. The increase in AR_{Cr} in counter-current mode can be explained by the increase in the coalescence phenomena. Indeed, in the counter-current mode, the lower bubble rising velocity causes higher gas holdup and, thus, the more compact arrangement of bubbles leads to higher coalescence rate (Besagni and Inzoli, 2016b, c). It is, therefore, easy to understand that the counter-current mode causes the increase in the critical value of the aspect ratio, AR_{Cr}.

3.2.2. Flow regime transitions

The first and the second flow regime transitions (as defined in Section 2.3.1) have been analyzed by applying the methods presented in Sections 2.3.2 and 2.3.3. Fig. 5b and d display the first and the second transition points and show the boundaries of the homogeneous, the transition and the heterogeneous flow regimes. In particular Fig. 5b displays the influence of *AR* on the transition gas velocities ($U_{G,trans,I}$ and $U_{G,trans,II}$) and Fig. 5d the influence of *AR* on the transition gas holdups ($\varepsilon_{G,trans,I}$ and $\varepsilon_{G,trans,II}$).

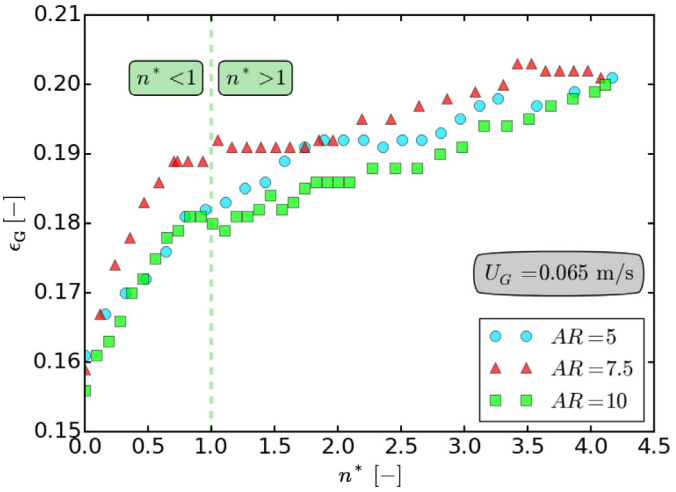

Fig. 7. Relation between NaCl concentration and gas holdup ($U_G = 0.065$ m/s).

The counter-current mode destabilizes the homogenous flow regime, compared with the batch mode, as the more compact arrangement of the bubbles leads to an earlier appearance of the "*coalescence-induced*" bubbles and, thus, the flow regime transition; the comprehensive discussion concerning the effect of the counter-current mode on the destabilization of the homogeneous flow regime can be found in Besagni and Inzoli (2016b, c). This observation is in agreement with the previous literature. Jin et al. (2010) have reported that the transition point is the same if U_L is lower than 0.04 m/s, whereas for higher U_L, the transition velocity decreases with increasing U_L. Otake et al. (1981) have observed an earlier flow regime transition increasing the liquid flowrate in the counter-current mode (U_L up to - 0.15 m/s). Similar conclusions have been drawn by Yamaguchi and Yamazaki (1982) ($d_c = 0.04$ m and 0.08 m) and in our previous research (Besagni et al., 2014; Besagni et al., 2016a; Besagni and Inzoli, 2016b, c). As expected from our experimental results in the batch mode, the homogeneous flow regime has been destabilized (decrease in $U_{G,trans,I}$ and $\varepsilon_{G,trans,I}$) while increasing *AR*, up to AR_{Cr}, in agreement with some of the previous studies (Ruzicka et al., 2001a; Sasaki et al., 2016; Zahradník et al., 1997). The reasons are the same as stated before: in short bubble columns the coalescence phenomena are more important, the liquid circulation patterns are not fully developed and the end-effects are more important. Similarly, the systems is likely to become fully heterogeneous (decrease in $U_{G,trans,II}$ and $\varepsilon_{G,trans,II}$) decreasing *AR*.

3.3. The effect of aspect ratio in non-coalescing (air-water-NaCl) systems

First, we have tested the effect of NaCl concentration on the gas holdup for fixed gas superficial velocity (Fig. 7) and, secondly, we have analyzed the influence of *AR* and NaCl concentration on the gas holdup curves (Figs. 7 and 8). Finally, the gas holdup measurements have bene used to evaluate the flow regime transitions (Fig. 10). It is worth noting that no crystallization inside the orifices on the plate has been observed (see ref. Orvalho et al., 2009)).

3.3.1. Gas holdup

Fig. 7 displays the influence of NaCl concentration on the gas holdup for fixed gas superficial velocity ($U_G = 0.065$ m/s) at three aspect ratios ($AR = 5$, 7.5 and 10). In Fig. 7 we have clearly distinguished between the "*coalescent flow regime*" ($n^* < 1$) and the "*non-coalescent flow regime*" ($n^* > 1$), through the dimensionless concentration, n^*, as defined in Eq. (2) and considering $n_t = 0.145$ mol/l, according to the experimental study of Zahradník et al. (1999) (as we have discussed in Section 2.1.2). In the "*non-coalescent flow regime*", a continuous increase of ε_G while increasing the electrolyte concentration has been observed: indeed, in this region, bubble coalescence is progressively reduced while increasing the electrolyte concentration. For better understanding this concept, the reader should refer to the previous literature concerning the effects of electrolytes on the bubble properties (i.e., the literature survey in Section 2.1.2) and, in particular, to the work of Firouzi et al. (2015), who have summarized the experimental data relating the percentage of coalescence to the concentration of NaCl. Taking into account the literature concerning the effects of electrolytes on bubble coalescence (i.e., the coalescence between bubble pairs) and interfacial properties (i.e., the liquid film drainage), the relations between the bubble properties (the "*bubble-scale*") and the gas holdup (the "*reactor-scale*") can be understood. Indeed, the reduced coalescence rate shifts the bubble size distribution towards smaller bubbles: the small bubbles, having a positive lift coefficient (Tomiyama et al., 2002), spread in the cross-section of the column and reduce the liquid phase recirculation (Lucas et al., 2006; Lucas et al., 2005) so that no larger vorticities are expected, thus increasing ε_G. This concept is in agreement with our experimental observations concerning ethanol non-coalescing solution (Besagni et al., 2016b). On the contrary, in the "*coalescent flow regime*", a plateau has been observed and, subsequently, an increase until the maximum concentration, at approximately $n^* \approx 4$, where the three different curves converge to the same value of the gas holdup, because of the limit in salt solubility (see, for example, ref. Haynes, 2014). This result supports the existence of the dual effect of inorganic active compounds on bubble column fluid dynamics, as described by Orvalho et al. (2009). For a more detailed discussion concerning the dual effects in bubble columns, the reader should refer to ref. Besagni et al. (2017).

Fig. 7 displays the gas holdup curves for the different aspect ratios (in the range $5 \leq AR \leq 12.5$) and the different NaCl concentrations (in the range $0.14 < n^* < 3.64$, depending on the *AR*). Fig. 7a displays the experimental data ($AR = 12.5$) presented in our previous paper (Besagni and Inzoli, 2015), whereas Fig. 7b–d display the experimental data obtained in this experimental campaign. It is worth noting that the data obtained in our previous paper are slightly below the actual measurements. Indeed, despite the great care in the experimentations, some factors may, of course, affect the experimental results, especially in a large-scale experimental facility: (i) the quality of water may differ from day to day; (ii) minor residues of used liquids; (iii) minor changes in the temperature (the temperature is controlled within the range of 1 K, Section 2.1.1), (iii). The gas holdup grows continuously (and non linearly) while increasing the electrolyte concentration (in agreement with Ribeiro and Mewes, 2007; Zahradník et al., 1997), up to a certain value of the NaCl concentration (as also observed by Zahradník et al., 1999): this value of the NaCl concentration, is in agreement with the critical value of $n_t = 0.145$ mol/l, previously defined in this work. Please note that $n_t = 0.145$ mol/l has been selected following the study of Zahradník et al. (1999) and has been obtained using consideration from coalescence behavior of bubble pairs; currently, there is no agreement of the general value of n_t and a certain variability around this value is likely to be expected (Firouzi et al., 2015). However, it is clear that, the "*bubble-scale*" can be related to the bubble column scale (the "*reactor-scale*") by using the transition concentration, i.e., by using a theoretical approach as in Eq. (2). The non-linearity of the electrolytes effect upon the gas holdup, as discussed by Ribeiro and Mewes (2007) and in our previous paper (Besagni and Inzoli, 2015). The non-linearity of the electrolytes effect upon the gas holdup suggest that the fluid dynamics in bubble columns having a binary liquid phase can not be

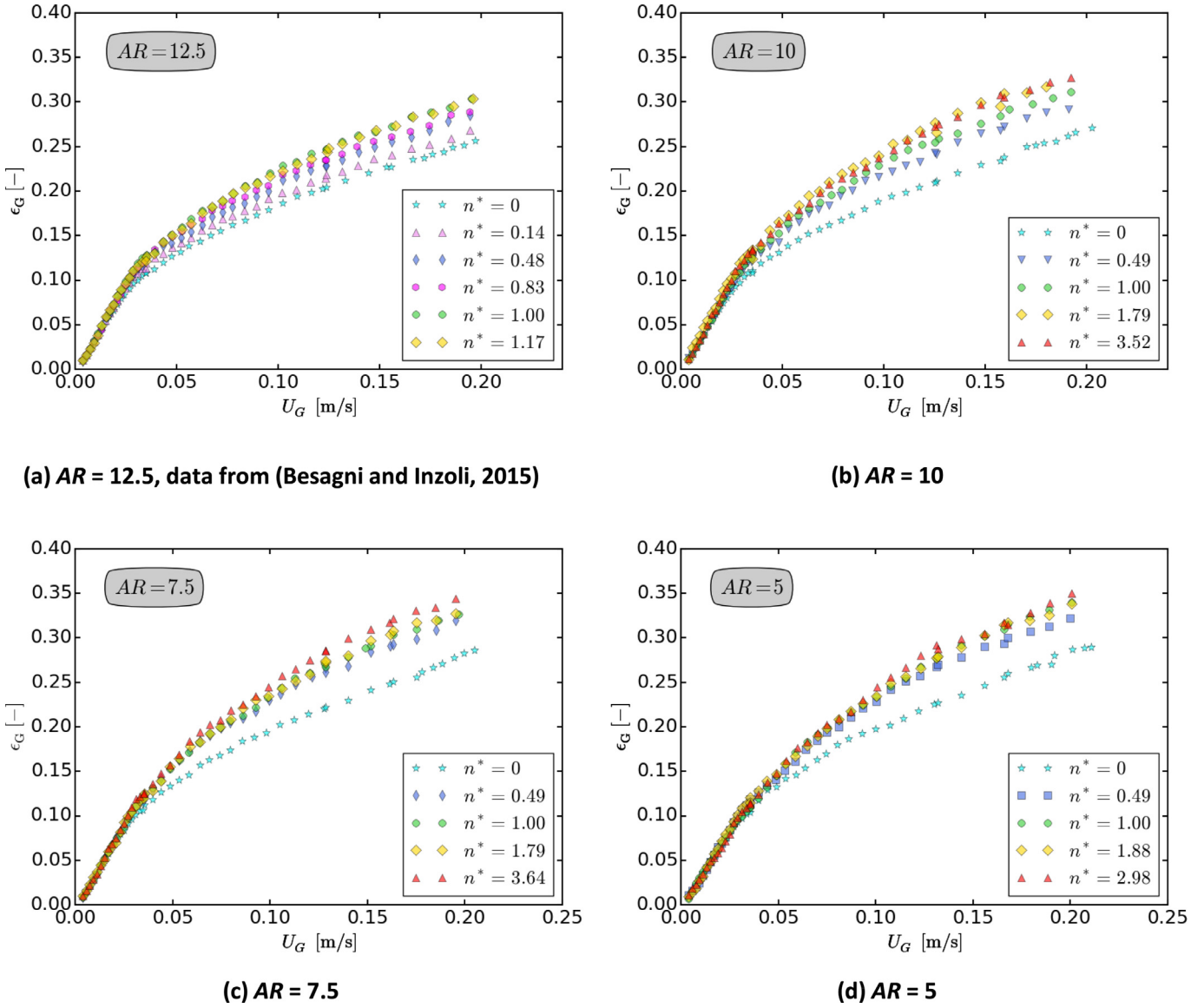

Fig. 8. Gas holdup measurements: air-water-NaCl system (influence of NaCl concentration).

entirely explained and modelled by using the bulk physical properties of the liquid phase (i.e., the surface tension, density and liquid phase viscosity); instead, the properties of the interface should be considered (i.e., as described by Eq. (2)). Fig. 9 displays the influence of the aspect ratios on the gas holdups, for fixed electrolyte concentrations. As already discussed, the measurements obtained at AR = 12.5 are slightly below the experimental results obtained in this work. A lower effect of *AR* on ε_G has been observed when using non-coalescing solutions. These results have clearly demonstrated how coalescence phenomena strongly affect the influence of *AR* on the bubble column fluid dynamics.

3.3.2. Flow regime transitions

The first and the second flow regime transitions (as defined in Section 2.3.1) have been analyzed by applying the methods presented in Sections 2.3.2 and 2.3.3. However, in the case of non-coalescing systems, the second flow regime transition points have been estimated to be very close to the first flow regime transition point: when using non-coalescing solutions, the boundaries of the transition flow regime become narrower and a quick transition from the homogeneous flow regime towards the heterogeneous flow regime happens. It is wort noting that, when using non-coalescing solutions, the coalescence suppression inhibits the appearance of "*coalescence-induced*" bubbles (as observed in the air-water system); on the contrary, cluster of small bubbles rise the column together. A similar behavior has been observed in air-water-ethanol non-coalescing solutions (Besagni et al., 2016b).

Fig. 10a displays the influence of *AR* on the transition gas velocities ($U_{G,trans,I}$) and Fig. 10b the influence of *AR* on the transition gas holdups ($\varepsilon_{G,trans,I}$). Please notice that, in Fig. 10, the experimental data corresponding to *AR* = 12.5 refers to the measurements presented in our previous paper (Besagni and Inzoli, 2015), whereas the experimental data at *AR* = 10, 7.5 and 5 to the measurements presented in this experimental campaign. It is worth noting that In Fig. 10, similarly to Fig. 7, we have clearly distinguished between the "*coalescent flow regime*" ($n^* < 1$) and the "*non-coalescent flow regime*" ($n^* > 1$), through the dimensionless concentration, n^*. In the "*non-coalescent flow regime*", the homogeneous flow regime is progressively stabilized while increasing the electrolyte concentration ($U_{G,trans,I}$ and $\varepsilon_{G,trans,I}$ increase almost linearly with n^*), which is caused by the inhibition of the coalescence. Indeed, in this region, the bubble coalescence is progressively reduced while

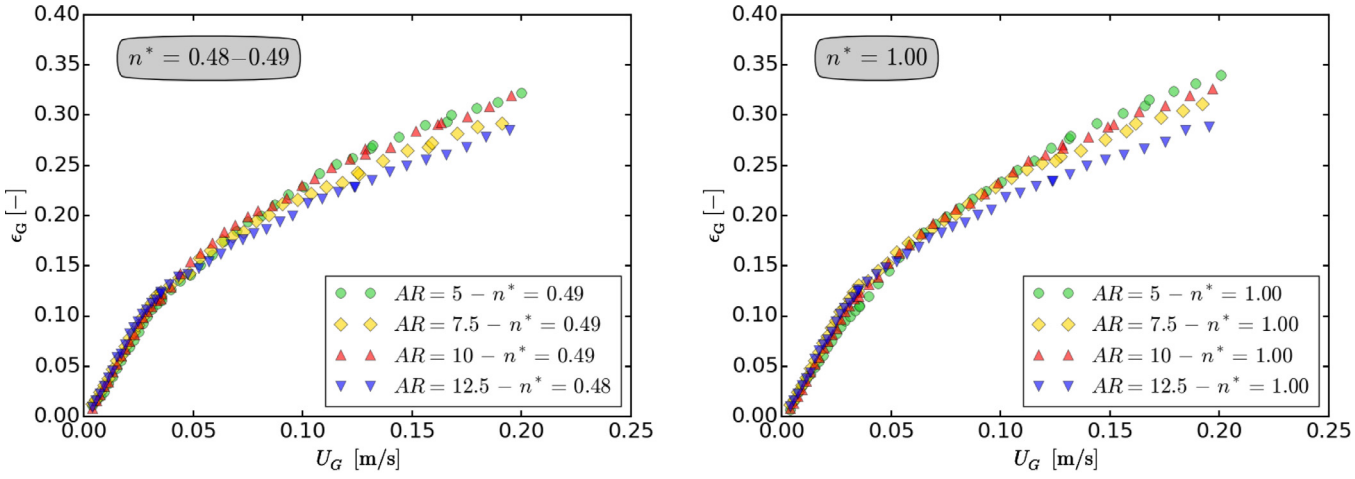

(a) Influence of *AR* on ε_G (n^* = 0.48 – 0.49) **(b) Influence of *AR* on ε_G (n^* = 1.00)**

Fig. 9. Gas holdup measurements: air-water-NaCl system (influence of AR).

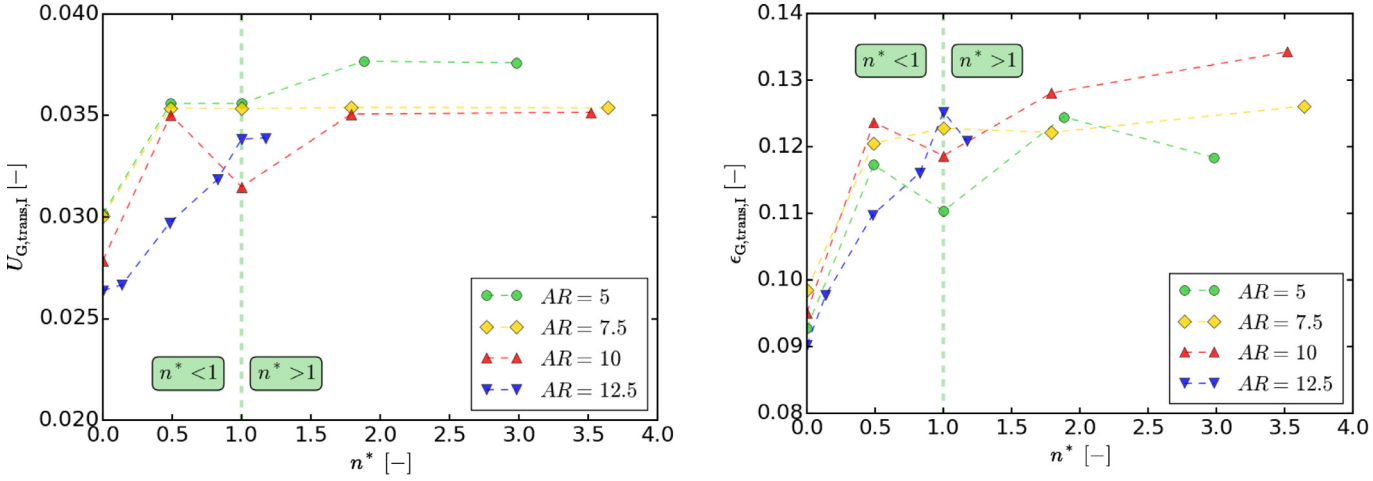

(a) Influence of *AR* and *n on $U_{G,trans,I}$** **(b) Influence of *AR* and *n** on $\varepsilon_{G,trans,I}$**

Fig. 10. Flow regime transitions: air-water-NaCl system.

increasing the electrolyte concentration (up to a critical concentration, n_t), as verified by different authors and summarized by Firouzi et al. (2015) (see also Section 3.3.1). The electrolytes reduce the coalescence, rate, but do not affect largely the break-up rate: consequently, the number of small bubbles increases, thus stabilizing the homogeneous flow regime by the mechanisms described by Lucas et al. (2006, 2005). Notice that the mechanisms that stabilize the homogeneous flow regime are similar to the ones supposed to increase the gas holdup. Therefore, the results suggest that the changes in the bubble-scale (which turns into changes of the bubble size distributions) stabilize/destabilize the homogeneous flow regime and, thus, increase/decrease the gas holdup, as previously observed in our paper concerning the influence of ethanol (Besagni et al., 2016b).

4. The gas holdup correlation

The aim of this section is to fill the gap in the literature concerning the lack of gas holdup correlations considering the influence of (i) *AR* and (ii) U_L and (iii) the liquid phase properties (in this case, the electrolytes). The many relations between the bubble column fluid-dynamic parameters and the variables characterizing the system make it difficult to find general correlations for the precise estimation of the gas holdup curve, which is the analytical relation between U_G and ε_G ($\varepsilon_G = f(U_G)$). Numerous correlations are available in literature, although due to the fluid dynamic complexity of the problem none of them can be either considered of general validity or applied to a wide range of geometrical parameters and operating conditions. A large set of available correlations have been tested against our experimental datasets and have shown low accuracy in predicting the experimental gas holdup throughout the operating range, as observed by Besagni and Inzoli (2016b, c) and De Guido et al. (2016).

In order to propose a new correlation, firstly, a scheme of correlation must be selected. Generally speaking, a general correlation for the gas holdup would be function of the different parameters characterizing the system:

$$\varepsilon_G = f(U_G, U_L, \mu_L, \mu_G, \rho_L, \rho_G, \sigma, d_c, H_0, d_o, g, \ldots) \quad (19)$$

It should be noted that the global and local flow properties depend on the prevailing flow regimes and a gas holdup correlation should take into account, at least, the first flow regime transition (i.e., $U_{G,trans,I}$). Therefore, the main concept in this study is to pro-

pose a new scheme for gas holdup correlations based on the flow regime transition point. This concept has the underlying assumption that systems having similar flow regime transition points behave similarly on a global point of view (as also stated in Besagni and Inzoli, 2016b). Taking into account this concept and the goals of this study (propose a correlation able to consider the effect of *AR*, U_L and electrolytes on the gas holdup), from Eq. (19) follows Eq. (20):

$$\varepsilon_G = f(d_c, d_o, U_G, U_{G,trans,I}, U_L, AR, n/n_t) \tag{20}$$

Moreover, considering a large-diameter bubble column, the wall effects can be neglected. In addition, if considering a "coarse" gas sparger, it follows that the influence of the gas sparger openings can be neglected.[4] The former consideration is related to "criterion 1'' and the latter to "criterion 3'' of the Wilkinson scale-up criteria. Therefore, from Eq. (20) follows Eq. (21):

$$\varepsilon_G = f(U_G, U_{G,trans,I}, U_L, AR, n/n_t) \tag{21}$$

Where the effects of the electrolytes have been taken into account through the ratio between the molar and the critical concentrations (n/n_t), as described in Section 2.1.2 and in Section 3.3, thus relating the "*bubble-scale*" to the "*reactor-scale*". In the following, Eq. (21) is further elaborated and its analytical forms are proposed. At first, a new gas holdup correlation has been assessed for the batch mode (Section 4.1) and, subsequently, it is extended for the counter-current mode (Section 4.2) and, finally, to account for the presence of electrolytes (Section 4.3). The extension of the correlation to the counter-current mode and to electrolytes is obtained starting from the analysis of the experimental results and their physical interpretation, while keeping the number of the needed empirical constants as lowest as possible, to avoid complicated formulations.

4.1. Gas holdup correlation for coalescing (air-water) systems: batch mode

The starting point to develop our correlation is the recent study of Sasaki et al. (2016), who have proposed the very first gas holdup correlation to take into account the influence of *AR*; in particular, the authors have related the gas holdup to H_0, through the Froude number, *Fr* (where $Fr = U_G/(gH_0)$):

$$\varepsilon_G = max\left[\frac{A_1^{R1} Fr}{1 + A_2^{R1} Fr}, \frac{A_1^{R2} Fr}{1 + A_2^{R2} Fr}\right] \tag{22}$$

Where the constants ($A_1{}^{R1}$, $A_1{}^{R2}$, $A_2{}^{R1}$ and $A_2{}^{R2}$) should be fitted cases by cases (i.e., column design, liquid and gas phases, etc....) and, for the circular bubble column of Sasaki et al. (2016) they are as follows: $A_1{}^{R1} = 10.6$, $A_1{}^{R2} = 7.7$, $A_2{}^{R1} = 19.9$ and $A_2{}^{R2} = 11.4$; the subscripts R^1 and R^2 refer to the homogeneous and heterogeneous flow regimes, respectively (the flow regime transition is, thus, accounted by using different values of the constants).

Figs. 11 and 12 compare our experimental measurements (Fig. 3a) and the literature gas holdup data (Fig. 3) with the values predicted by Eq. (22): Eq. (22) fits fairly well the data at low *AR up to* $AR = AR_{Cr} = 5$, while the error increases for higher *AR* (i.e., Fig. 12b and d). In particular, Eq. (22) is unable to predict the stabilization of the gas holdup above the critical aspect ratio, AR_{Cr}. Because of these limitations in Eq. (22), the proposed correlation is based on the following considerations: (i) the same structure of the correlation by Sasaki et al. (2016) has been used and (ii) considering the flow regime transition point (thus avoiding variable constants, as in Eq. (22)). In particular, the flow regime transition point has been accounted by using the dimensionless gas velocity ($U_G{}^*$), defined as follows:

$$U_G^* = U_G/U_{G,trans,I} \tag{23}$$

Therefore, Eq. (21), for the air-water system in the batch mode, considering Eq. (23) reduces to Eq. (24):

$$\varepsilon_G(U_G, U_{G,trans,I}, U_L, AR, n/n_t) \xrightarrow{U_L=0, Air-water} \varepsilon_G(U_G, U_{G,trans,I}, AR) \xrightarrow{Eq.(23)} \xrightarrow{Eq.(23)} \varepsilon_G(U_G/U_{G,trans,I}, AR) = \varepsilon_G(U_G^* AR) = \frac{C_1 U_G^*}{1 + C_2 U_G^*} AR^{C3} \tag{24}$$

Where $U_{G,trans,I}$ has been estimated by regressing our experimental measurements (Fig. 3a):

$$U_{G,trans,I} = 0.0324AR - 0.0004 \tag{25}$$

The three constants in Eq. (24) (C_1, C_2 and C_3) have been computed through the minimization of the square of the errors, by comparing Eq. (25) against our experimental dataset (Fig. 3a): $C_1 = 0.1749$, $C_2 = 0.2876$ and $C_2 = -0.2$. The proposed correlation has been tested against our dataset and the data from the literature (Fig. 4) and is compared with the correlation proposed by Sasaki et al. (2016). The results are summarized in Figs. 11 and 12. Eq. (24) predicts fairly well the experimental data in the investigated range; in particular, Eq. (24) is able to predict the gas holdup shape beyond the critical aspect ratio AR_{Cr} and performs generally better compared with Eq. (22), except for the experimental data of Sasaki et al. (2016), upon which the constants in Eq. (22) have been calibrated. In particular, Eqs. (22) and (24) are further compared by checking the errors (defined in the following by Eqs. (26),(27) and (28)) between the experimental data and the data. In particular, Eq. (26) represents the sum of squared residuals between the experimental data and the correlation outputs:

$$error = \sum_{i=1}^{N_{data}} \left(\varepsilon_{G,i,experimental} - \varepsilon_{G,i,correlation}\right)^2 \tag{26}$$

Where *i* is the data considered in the dataset and N_{data} the total number of data. Another method allowing a comparison for correlation performances is mean percentage error (*MPE*) defined as follows:

$$MPE = \frac{100\%}{N_{data}} \sum_{i=1}^{N_{data}} \frac{\varepsilon_{G,i,experimental} - \varepsilon_{G,i,correlation}}{\varepsilon_{G,i,experimental}} \tag{27}$$

Mean absolute percentage error (*MAPE*) should also be considered, otherwise some outcomes may turn out to be biased. The formula reads as follows:

$$MAPE = \frac{100\%}{N_{data}} \sum_{i=1}^{N_{data}} \frac{\left|\varepsilon_{G,i,exp} - \varepsilon_{G,i,correlation}\right|}{\varepsilon_{G,i,exp}} \tag{28}$$

The result of the analysis and the summary of the errors are proposed in Table 2. As clearly observed, our correlations performs better compared with the one by Sasaki et al. (2016). The overall good performance of Eq. (24) compared with Eq. (22) are related to (i) the calibration of the constants (C_1, C_2 and C_3) upon an experimental dataset, related to a bubble column with large diameter and large gas sparger opening (Wilkinson et al., 1992); (ii) the physical meaning underlying the correlation, which is based on the transition point.

4.2. Gas holdup correlation for coalescing (air-water) systems: counter-current mode

In this section, Eq. (24) has been extended to take into account the counter-current mode. In a previous study, some of the authors have tested different scheme of correlations to relate the gas holdup in the batch mode to the gas holdup in the counter-current

[4] Please note that a more rigorous formulation of Eq. (19) would require a non-dimensional formulation of the bubble column diameter and sparger opening

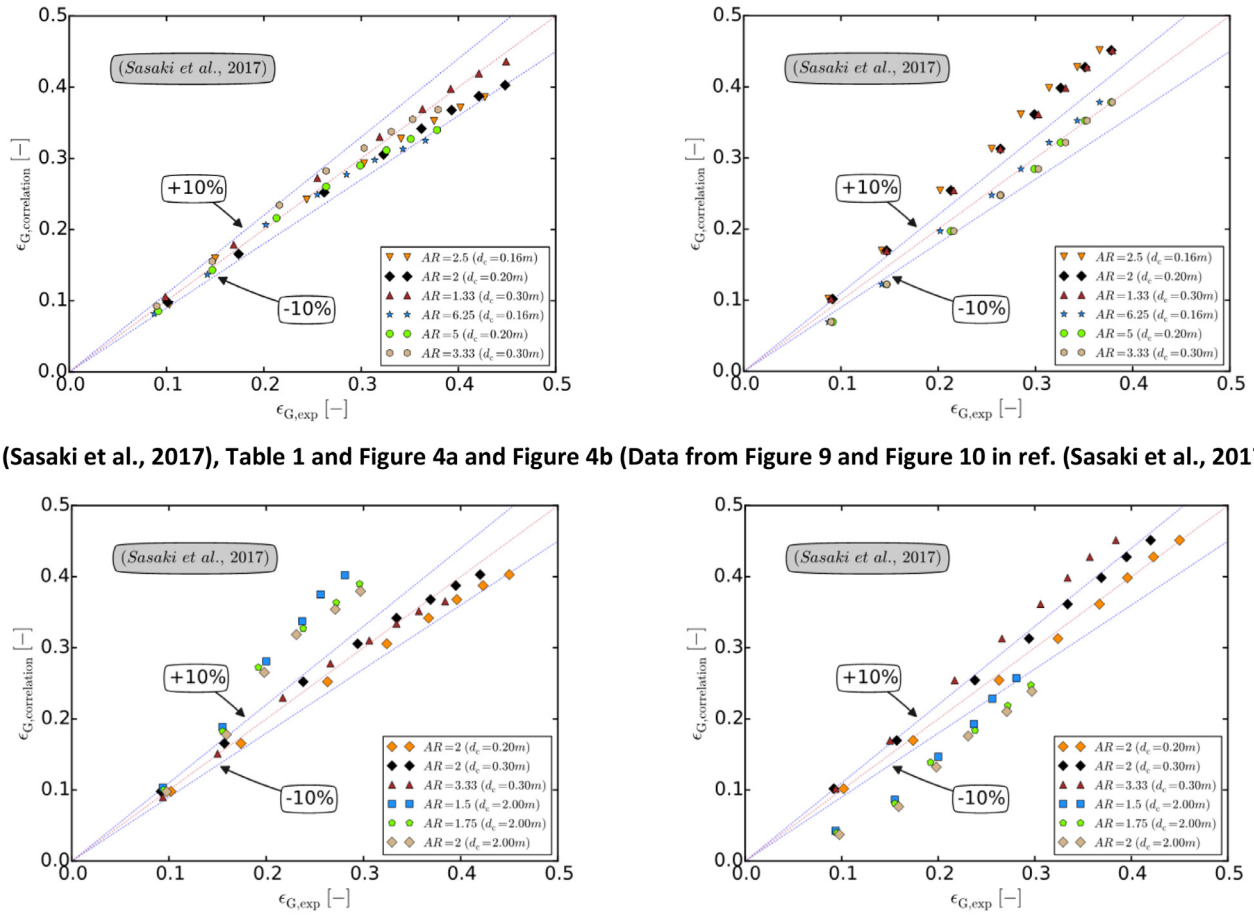

Fig. 11. Comparison between experimental data (air-water system in batch mode) and correlations: proposed correlation and correlation from Sasaki et al. (2016) - Part A.

mode (De Guido et al., 2016). Among the different approaches tested, the following analytical form seems to be promising:

$$\varepsilon_G = \frac{U_G}{\frac{U_G}{\varepsilon_{G,Batch}} - \gamma \frac{U_L}{1-\varepsilon_{G,Counter-Current}}} \tag{29}$$

The reader should refer to the discussion proposed by De Guido et al. (2016) for further information concerning correlations for counter-current bubble columns. Eq. (29) allows the evaluation of the gas holdup in the batch mode for given counter-current gas holdup, superficial gas and liquid velocity, and vice-versa. Moreover, if $U_L = 0$ m/s, the gas holdup can computed as a function of U_G with the correlation previously proposed for the batch mode (Eq. (24)) as follows:

$$\varepsilon_G = \frac{U_G}{\frac{U_G}{\varepsilon_{G,Batch}} - \gamma \frac{U_L}{1-\varepsilon_{G,Counter-Current}}} \overset{U_L=0}{\rightarrow} \frac{U_G}{\frac{U_G}{\varepsilon_{G,Batch}}} = \varepsilon_{G,Batch} \tag{30}$$

De Guido et al. (2016) have estimated $\gamma = 0.58$ by the minimization of the sum of absolute deviations between calculated and experimental gas holdups (the dataset used was: Besagni and Inzoli (2016b, c)). To improve the performance of Eq. (29) achieved by De Guido et al. (2016), and to extend its range of validity, γ should be considered function of AR and U_L. To this end, we have employed both the datasets obtained in this study (influence of AR, fixed U_L) as well as the ones proposed in our previous papers (Besagni et al., 2016a; Besagni and Inzoli, 2016b, c) (influence of U_L, fixed AR):

- the experimental results presented in this work ($U_L = -0.0864$ m/s, $5 < AR < 15$, Fig. 3b). The values of γ as a function of AR have been computed by minimization of the sum of squared residuals between correlation and experimental data (Fig. 13a); subsequently, Eq. (31) has been selected to fit the data:

$$\gamma(AR)|_{U_L=-0.0846} = -0.058AR + 1.14 \tag{31}$$

- the experimental results presented in our previous papers ($5 < U_L < 15$ m/s, $AR = 12.5$): the (i) spider-gas sparger bubble column (Besagni and Inzoli, 2016b) and the (ii) annular gap bubble column with pipe gas sparger (Besagni et al., 2016a; Besagni and Inzoli, 2016c). The values of γ as a function of U_L have been computed by minimization of the sum of squared residuals between correlation and experimental data (Fig. 13b); subsequently, Eq. (32) has been selected to fit the data:

$$\gamma(U_L)|_{AR=12.5} = -1.524|U_L| + 0.596 \tag{32}$$

Where, $|U_L|$ is the numerical value of U_L, without units, so that γ is still non-dimensional.

Fig. 14a compares the predicted gas holdup against the experimental measurements obtained in this research, whereas Fig. 14b and Fig. 14c compare the predicted gas holdup against the experimental measurements obtained in our previous papers. Eq. (29) is able to predict fairly well the experimental data, with a relative error lower than 10%, in the heterogeneous flow regime (the re-

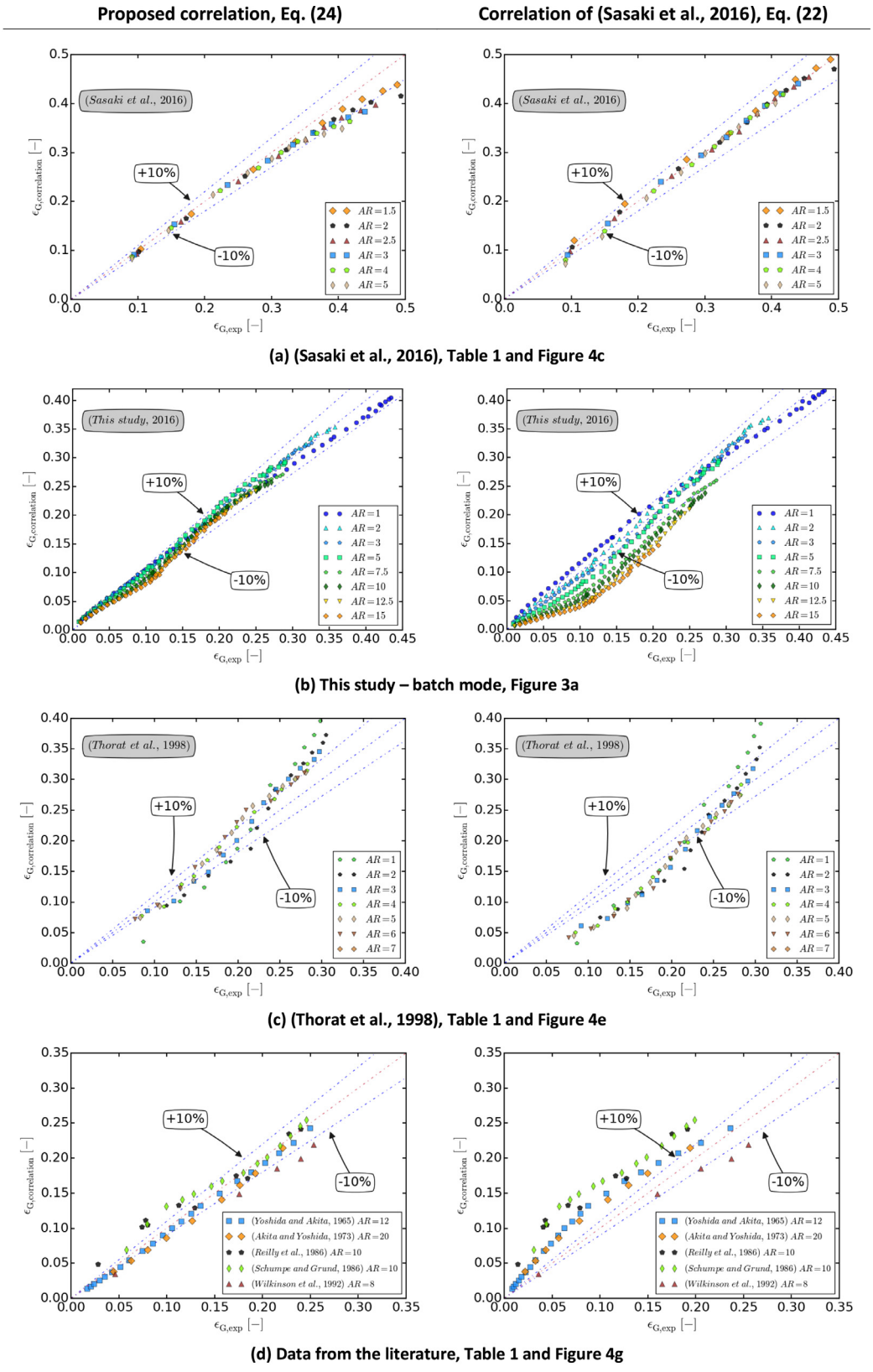

Fig. 12. Comparison between experimental data (air-water system in batch mode) and correlations: proposed correlation and correlation from Sasaki et al. (2016) - Part B.

Table 2
Comparison between prediction of Eqs. (22) and (24): errors evaluated based on Eqs. (26–28).

Ref.	AR [-]	d_C [m]	This Study, Eq. (24)			(Sasaki et al., 2016), Eq. (22)		
			SSR	MPE	MAPE	SSR	MPE	MAPE
This study	1	0.24	0.01103	-3.7%	8.6%	0.01095	-11.5%	14.5%
This study	2	0.24	0.00468	-10.5%	10.5%	0.002	-7.5%	7.8%
This study	3	0.24	0.00235	-9.1%	9.1%	0.00245	0.8%	6.3%
This study	5	0.24	0.00497	-9.4%	9.4%	0.0089	9.6%	11.4%
This study	7.5	0.24	0.00126	-1.4%	4.9%	0.04349	23.2%	23.2%
This study	10	0.24	0.00189	2.0%	5.4%	0.06942	30.6%	30.6%
This study	12.5	0.24	0.00395	4.4%	8.4%	0.09773	38.2%	38.2%
This study	15	0.24	0.00467	7.5%	10.3%	0.09823	47.5%	47.5%
(Sasaki et al., 2017)	2	0.2	0.00545	6.4%	6.4%	0.04662	-34.1%	34.1%
(Sasaki et al., 2017)	2	0.3	0.00086	-2.3%	3.9%	0.03239	-28.1%	28.1%
(Sasaki et al., 2017)	2.3	0.3	0.00072	-0.2%	2.9%	0.02623	-23.7%	23.7%
(Sasaki et al., 2017)	1.5	2	0.00028	1.1%	1.6%	0.01340	27.2%	27.2%
(Sasaki et al., 2017)	1.8	2	0.00457	-8.0%	8.0%	0.01943	32.0%	32.0%
(Sasaki et al., 2017)	2	2	0.02084	-16.4%	16.4%	0.02479	35.4%	35.4%
(Sasaki et al., 2017)	2.5	0.16	0.00359	4.2%	5.7%	0.03454	-23.3%	23.3%
(Sasaki et al., 2017)	1.3	0.3	0.00081	-2.9%	3.7%	0.02333	-18.1%	18.1%
(Sasaki et al., 2017)	6.3	0.2	0.00044	3.0%	3.8%	0.00084	6.2%	7.0%
(Sasaki et al., 2017)	5	2	0.00037	2.8%	3.3%	0.00182	10.1%	10.1%
(Sasaki et al., 2017)	3.3	0.3	0.00092	-5.0%	5.0%	0.00206	10.5%	10.5%
(Sasaki et al., 2016)	1.5	0.2	0.00535	4.7%	4.7%	0.0013	-4.6%	4.6%
(Sasaki et al., 2016)	2	0.2	0.01066	6.7%	6.7%	0.0007	-1.2%	2.4%
(Sasaki et al., 2016)	2.5	0.2	0.00817	6.7%	6.7%	0.00014	0.0%	0.9%
(Sasaki et al., 2016)	3	0.2	0.00655	6.7%	5.3%	0.00013	0.0%	1.2%
(Sasaki et al., 2016)	4	0.2	0.00582	5.6%	5.6%	0.00029	2.1%	2.7%
(Sasaki et al., 2016)	5	0.2	0.00581	5.7%	6.0%	0.00071	4.0%	4.3%
(Thorat et al. 1998)	1	0.385	0.05533	-8.1%	25.2%	0.03389	-0.1%	22.5%
(Thorat et al., 1998)	2	0.385	0.02034	1.5%	18.7%	0.01845	13.5%	20.8%
(Thorat et al., 1998)	3	0.385	0.01157	1.2%	15.8%	0.01372	17.9%	20.7%
(Thorat et al., 1998)	4	0.385	0.00769	-0.3%	13.8%	0.0127	20.7%	21.6%
(Thorat et al., 1998)	5	0.385	0.0084	-1.0%	14.6%	0.01514	22.8%	23.1%
(Thorat et al., 1998)	6	0.385	0.00806	-3.3%	12.9%	0.01464	23.6%	23.6%
(Thorat et al., 1998)	7	0.385	0.00687	-0.9%	15.0%	0.01924	26.9%	26.9%
(Wilkinson et al., 1992)	8	0.158	0.00455	-20.5%	20.5%	0.00322	-11.4%	11.4%
(Reilley et al., 1986)	10	0.3	0.00359	2.3%	13.7%	0.03185	10.4%	18.7%
(Schumpe and Grund, 1986)	10	0.3	0.00345	8.5%	8.8%	0.05143	37.9%	37.9%
(Yoshida and Akita, 1965)	12	0.301	0.00084	-8.3%	8.3%	0.01814	30.5%	30.7%
(Akita and Yoshida, 1973)	20	0.152	0.00131	-11.9%	11.9%	0.00638	26.4%	26.4%

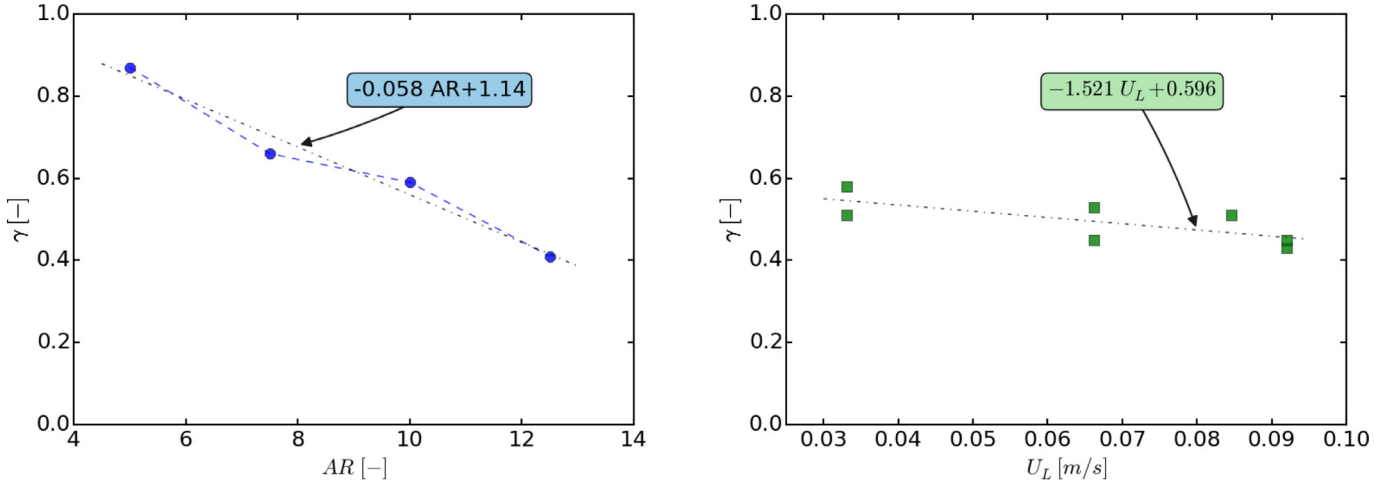

(a) *Relation between γ and AR* **(b) *Relation between γ and U_L***

Fig. 13. Relations between γ and the variables of the system in counter-current mode.

gion of interest for the industrial applications, see refs. Leonard et al., 2015; Rollbusch et al., 2015b). However, the performance of Eq. (29) decreases as U_L increases, while the agreement is better for lower values of U_L. This suggests that Eq. (29) is suitable for low liquid velocities and it is unable to predict the change of shape of the gas holdup curve near the flow regime transition point. Despite these limitations, to the author's best knowledge, Eq. (29) is the best available correlation to consider the counter-current mode; furthermore, it is an improved version of the scheme of correlation presented by De Guido et al. (2016). Further study would be devoted to improve the performance of Eq. (29), by more advanced variable formulation of γ and by improving the mathematical structure of Eq. (29).

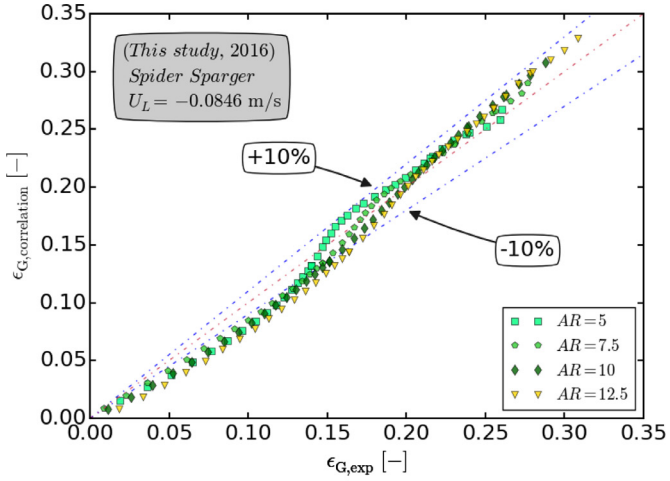

(a) This study: counter-current mode (Figure 2b)

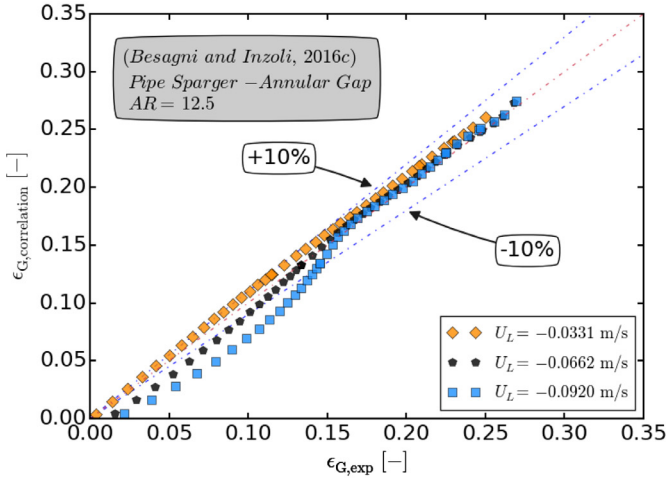

(b) Annular gap (Besagni and Inzoli, 2016c)

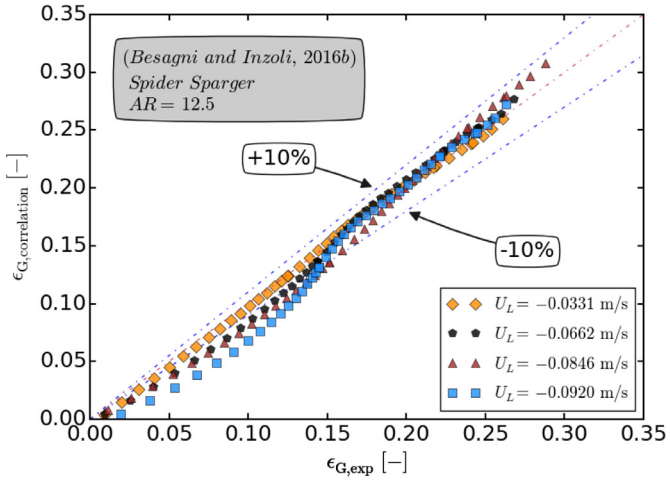

(c) Spider sparger (Besagni and Inzoli, 2016b)

Fig. 14. Comparison between experimental data (air-water system in counter-current mode) and the proposed correlation.

4.3. Gas holdup correlation for non-coalescing (air-water-NaCl) systems

The gas holdup grows continuously while increasing the electrolyte concentration (Fig. 7, Section 3.3.1). Therefore, it is reasonably to modify the gas holdup correlation for the air-water system (Eq. (24)), by including an additional parameter. This parameter should provide an insight in the nature of the system, thus having a more general interpretation rather than this experimental work. In this respect, Ribeiro and Mewes (2007) have obtained similar gas holdup curves regardless of the electrolyte for given dimensionless concentration n^*. Therefore, it follows that, a correlation employing n_t can be thought as of general validity in terms of the electrolyte nature. In particular, in this work, the functional form used to account for n^* is an exponential.

Therefore, Eq. (21), for the air-water-NaCl system in the batch mode, considering Eq. (2) reduces to Eq. (33) (it is worth noting that, when $n^* = 0$, Eq. (33) is no not more valid and Eq. (24) should be used):

$$\varepsilon_G(U_G, U_{G,trans,I}, U_L, AR, n/n_t) \xrightarrow{U_L=0} \varepsilon_G(U_G, U_{G,trans,I}, AR, n/n_t) \xrightarrow{Eq.(2),Eq.(23)} \xrightarrow{Eq.(2),Eq.(23)} \varepsilon_G\left(U_G^*, AR, \mathrm{n}/\left\{1.18\left(\frac{B\sigma}{r_b}\right)^{0.5} R_g T \left(\frac{\partial\sigma}{\partial n}\right)^{-2}\right\}\right) = \varepsilon_G\left(U_G^*,\ AR, n^*\right) = \frac{C_4 U_G^*}{1+C_5 U_G^*} exp\{C_6 n^*\} AR^{C_7} \tag{33}$$

Where $U_{G,trans,I}$ has been estimated by regressing our experimental data obtained at $AR = 10$ (Fig. 10a):

$$U_{G,trans,I} = 0.00004\frac{n}{n_t} + 0.035 = 0.00004 n^* + 0.035 \tag{34}$$

The four constants in Eq. (33) (C_4, C_5, C_6 and C_7) have been computed through the minimization of the square of the errors, by comparing Eq. (33) against our experimental dataset obtained at $AR = 10$ (Fig. 7b): $C_4 = 0.2237$, $C_5 = 0.2876$ ($C_5 = C_2$, in Eq. (24)), $C_6 = 0.03273$ and $C_7 = -0.2$ ($C_7 = C_4$, in Eq. (24)). It is interesting that two out of the four constants are equal to the values obtained in the air-water correlation (Eq. (24)); in particular, the exponent of AR is the same. Please note that, in this study, the transition concentration n_t has been selected following the study of Zahradnıḱ et al. (1999), $n_t = 0.145$ mol/l, as deeply discussed in Section 2.1.2. Of course, in general, Eq. (2) can used to estimate n_t modelling parameter to account for the chemical nature of electrolytes, by using the theoretical model of Prince and Blanch (1990) or future theoretical models that will be proposed in the future. Therefore, correlation proposed takes into account the modification at the "*bubble-scale*, when estimating the gas holdup. It is worth noting that the dataset obtained at $AR = 10$ has been used to ensure a calibration of (i) the four constants (C_4, C_5, C_6 and C_7) and (ii) the correlation for $U_{G,trans,I}$; $AR = 10$ have been selected because it is expected to be valid also for larger bubble columns, owing to the high AR value. Future studies will be devoted to propose modifications of Eq. (33) able to account for the simultaneous variation of electrolyte concentration and AR.

Fig. 15a compares the predicted gas holdup against the experimental measurements obtained in our previous paper ($AR = 12.5$, (Besagni and Inzoli, 2015)), whereas Fig. 15b–d compare the predicted gas holdup against the experimental measurements obtained in this experimental work ($AR = 5$, 7.5 and 10, Section 3.3.1). Eq. (33) has turned out to predict fairly well the gas holdup measurements at the different aspect ratios, with an error generally within ± 10%. The worst performance are observed at lower *ARs* (i.e., $AR = 5$, Fig. 15d), are mainly caused by the constants calibrated obtained at $AR = 10$, as expected. Following the recommendations of Ribeiro and Mewes (2007), we may conclude that the proposed

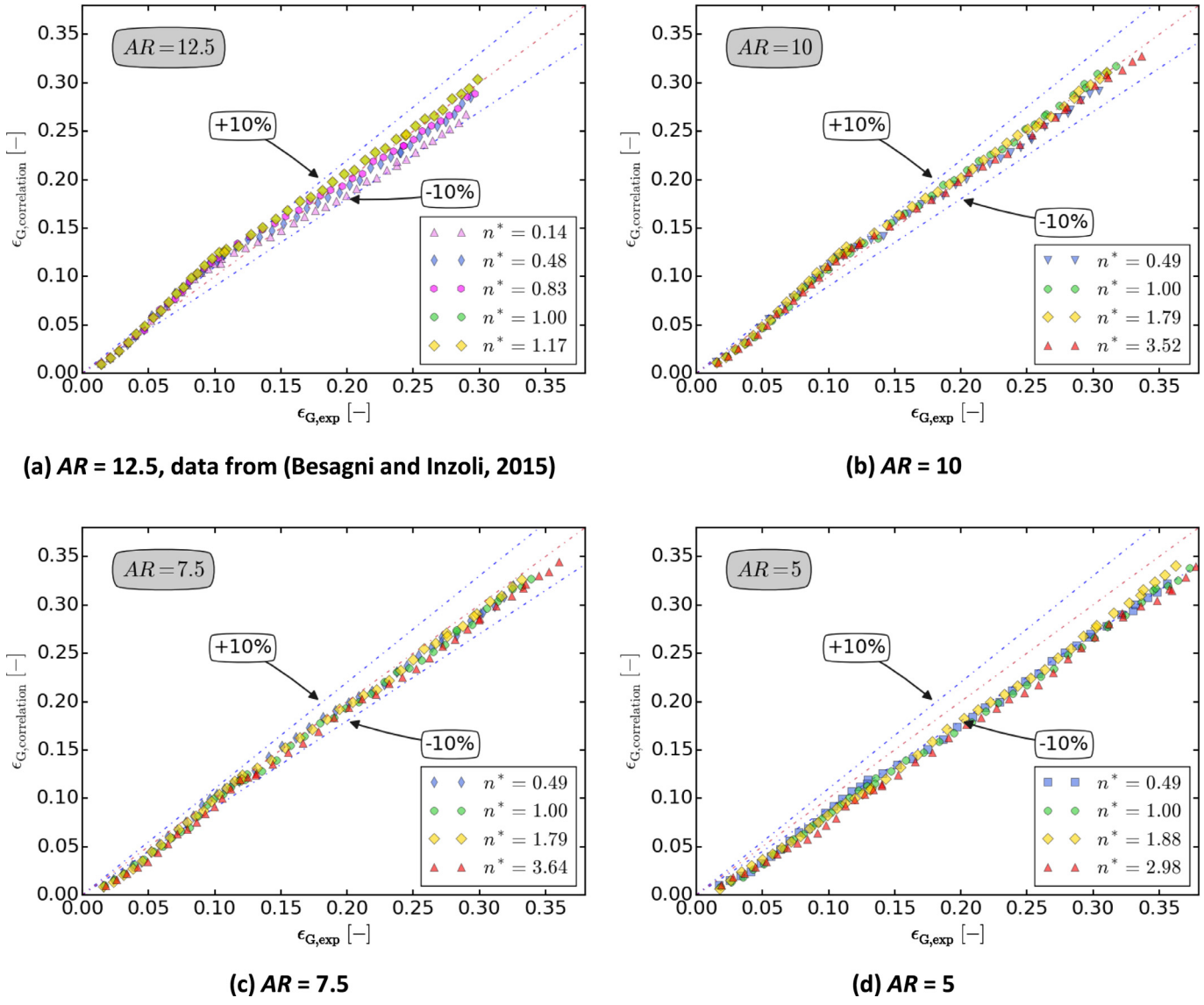

Fig. 15. Comparison between experimental data (air-water-NaCl system) and the proposed correlation.

correlation can be used to estimate the influence of electrolyte concentration regardless of the nature of the electrolyte itself.

5. Conclusions, outcomes and outlooks

5.1. Conclusions and outcomes

The gas holdup and flow regime transitions for the gas-liquid flow in a large-diameter bubble column have been investigated experimentally. The main results are summarized in the followings:

- **Air-water system in batch mode** (Section 3.1). Three flow regimes (the homogeneous flow regime, the transition flow regime, and the heterogeneous flow regime) have been identified, and the transition points between them have been evaluated. The aspect ratio, up to a critical value, has turned out to decrease the gas holdup and destabilize the homogeneous flow regime.
- **Air-water system in counter-current mode** (Section 3.2)**.** The counter-current mode has turned out to increase the gas holdup and destabilize the homogeneous flow regime;
- **Air-water-NaCl system in batch mode** (Section 3.3). The electrolytes have turned out to increase the gas holdup and stabilize the homogeneous flow regime, because of coalescence phenomena governing the influence of *AR* on bubble column fluid dynamics.
- **Critical value of the aspect ratio** (Sections 3.1–3.3). The critical value of the aspect ratio ranged between 5 and 10, depending on the bubble column operation (i.e., batch or counter-current modes) and liquid phase properties.
- **Gas holdup correlation** (Section 4). A new scheme of correlation for the prediction of the gas holdup: the correlation has been assessed for the batch mode (Eq. (24)) and is then extended for the counter-current mode (Eq. (30)) and the presence of electrolytes (Eq. (33)). Proper modifications have been introduced to extend the range of validity while keeping as low as possible the number of empirical constants. The correlation predicts fairly well the gas holdup measurements at the different aspect ratios, with an error generally within ± 10%.
- **Physical properties and interfacial properties.** The fluid dynamics in bubble columns having a binary liquid phase can not be entirely explained and modelled by using the bulk physical properties of the liquid phase (i.e., the surface tension, density and liquid phase viscosity); indeed, the properties of the interface should be considered (i.e., as described by Eq. (2)).

In conclusion, the present study has contributed to the existing discussion on the scale-up criteria and the bubble column de-

sign. The proposed scheme of correlation is particularly interesting to study the influence of the aspect ratio, operation mode and electrolyte concentration for a given experimental dataset. Furthermore, the proposed dataset would be useful to other researcher devoted to the study of bubble column fluid dynamics.

5.2. Outlooks

It has not escaped our notice that Sasaki et al. (2017) stated that *AR* is useless in evaluation of the critical height, above which the gas holdup does not depend on the initial liquid level. Conversely, we support the use of *AR* as scale-up criteria. It is worth noting that Sasaki et al. studied a very-large-diameter bubble column (having $d_c >> 0.15$ m; where, 0.15 m is the threshold value stated by criterion#1) and our experimental setup has $d_c = 0.24$ m > 0.15 m. Future researchers are encouraged to perform similar experimental investigations in very-large-diameter and high *AR* bubble column in order to clarify where our proposal or the proposal of Sasaki et al. (2017) is to be further pursued in future research. Unfortunately, our experimental setup is unable to perform such experimental investigation because of construction issues. This is a starting point for future studies, which will allow a much deeper knowledge on the topic, which is, up to these days, is not completely understood.

Acknowledgments

The paper is the results of the contribution and discussion by many people and the outcome of the last years of research. In particular, the authors would like to thank Sasaki and co-authors for their interesting and valuable study concerning the influence of the initial liquid level on the gas holdup and flow regime transitions, which has been the starting point to develop this work. The authors would like to thank the reviewers for their suggestions and point of view. We hope that the present work may serve to future researchers as starting point for the discussion of scale-up criteria in bubble columns. Scientific progress is a slow progress reasoned on undoubtedly arguments.

Appendix A. Gas holdup measurements: uncertainty assessment

Herein, the uncertainty analysis related to gas holdup measurements is presented. It is worth noting that the uncertainty related to the gas and liquid superficial velocities are the ones available from the flowmeters manufacturers and listed and discussed in Section 2.1. The gas holdup measurement uncertainty is related to the measurement of the free-surface level with respect to the reference gas sparger one. Indeed, the gas holdup is computed by using the bed expansion technique and, thus, two heights have to be measured (Eq. (3)): H_0 and H_D.

The uncertainty related to the evaluation of H_0 (ξ_{H0}) is related to the accuracy of the measurement apparatus (a) as follows:

$$\xi_{H_0} = \frac{a}{2\sqrt{3}} \tag{A.1}$$

Where, in the present case, $a = 1$ mm. For the purposes of this study, this kind of uncertainty will be neglected, as it yields deviations much smaller if compared to the following ones.

The evaluation of H_D is instead complicated by the oscillation of the free-surface level around its mean value as bubbles are vented to the outlet (especially when "*coalescence-induced*" bubbles appear). To quantify this contribution, a set of $l = 30$ measurements were performed for three representative gas superficial velocities ($U_G = 0.0188$, $U_G = 0.0393$, $U_G = 0.0903$ m/s). These values have been chosen as characteristic of (a) the onset of the transition flow regime, (b) the transition flow regime and (c) the heterogeneous flow regime. For every case considered, the mean value ($\overline{\varepsilon}$), the sample variance (s^2_{HD},) and the standard deviation (s_{H_D}) have been computed and the uncertainty have been assessed.

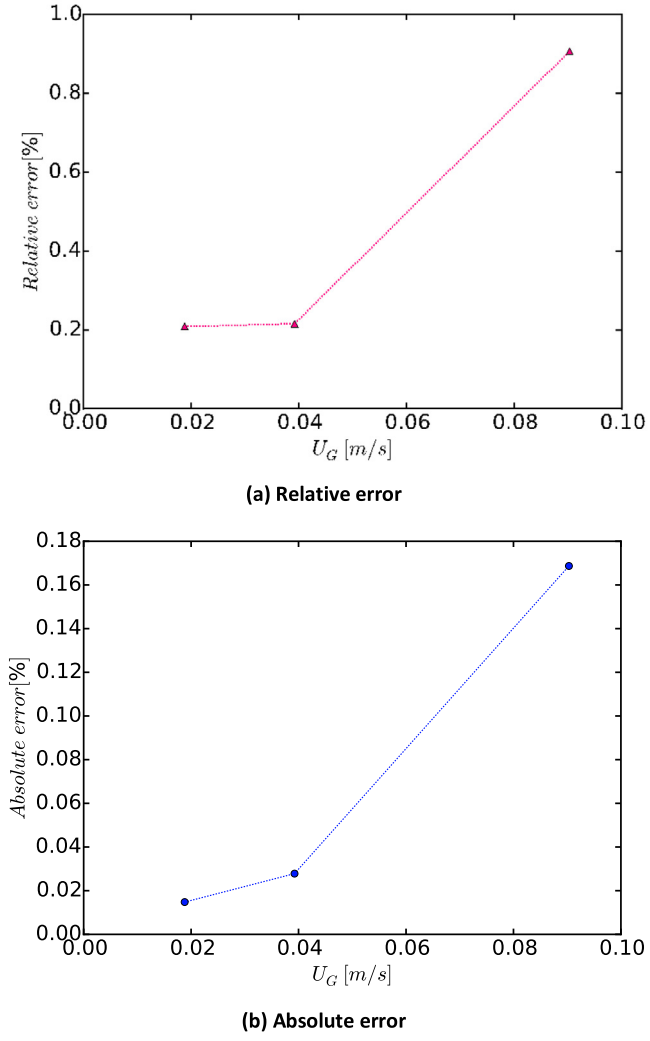

Fig. 16. Gas holdup measurements: uncertainty assessment.

Therefore, the reference gas holdup measurements can be reported with their respective ranges as:

$$\varepsilon_G = \overline{\varepsilon_G} \pm \frac{\Delta\varepsilon_G}{\sqrt{l}} \tag{A.2}$$

Where $\Delta\varepsilon$ reads as follows:

$$\Delta\varepsilon_G = \left| \frac{\partial \varepsilon_G(H_D)}{\partial H_D} \cdot s_{H_D} \right| \tag{A.3}$$

Where s_{HD} is the sample standard deviation for the liquid surface level measurements after the aeration mentioned before. By applying Eq. (A.3) the derivative can be computed and reads as follows:

$$\frac{\partial \varepsilon_G(H_D)}{\partial H_D} = \frac{\partial}{\partial H_D}\left(\frac{H_D - H_0}{H_D}\right) = \frac{H_0}{H_D^2} \tag{A.4}$$

It can be noticed that the above calculations have been performed considering H_0 as a constant, i.e. no uncertainty is taken into consideration about that parameter (as already discussed above).

Finally, from Eq. (A.4) and Eq. (A.3), Eq. (A.5) follows:

$$\Delta\varepsilon_G = \left| \frac{H_0}{H_D^2} \cdot s_{H_D} \right| \tag{A.5}$$

Result of such analysis are reported in Fig. 16 as relative and absolute error. It is possible to note that the dependence for the holdup measurement deviation on the gas superficial velocity is non-linear. Same reasoning can indeed be applied if expanded uncertainty should be considered.

Appendix B. Notes on the Wallis method

Herein, the detailed derivation of the Wallis method for the identification of the first flow regime transition point is proposed. This methods was firstly derived by Wallis (1969) in the early 1955 and, despite it is widely used in the literature, often there is confusion in its definition and equations. The goal of this section is to briefly propose the detailed derivation of the equations applied in this method, which may be helpful for future researchers.

At first, we start considering the two-phase from a local point of view and we define the volumetric flux. The flux is a vector quantity, but, in the following, it will be used to represent the scalar component in the direction of the motion along the vertical bubble column. The flux is related to the local gas holdup and to the local phase velocity, w, as follows:

$$J_L = (1-\varepsilon_G) w_L|_{Local} \tag{B.1}$$

$$J_G = \varepsilon_G w_G|_{Local} \tag{B.2}$$

The total local flux is, then, computed from Eq. (A.1) and Eq. (A.2) as follows:

$$J = J_L + J_G \tag{B.3}$$

The local volumetric fluxes are related to the volumetric flow rates (which is a quantity measured in the experimental setup, Q) as follows:

$$Q_L = \int J_L dA \tag{B.4}$$

$$Q_G = \int J_G dA \tag{B.5}$$

Before processing, it is worth reminding the definition of the superficial velocities (defined as the ration between the volumetric flow rates, Q, and the cross-sectional areas of the bubble column, A_c):

$$U_L = \frac{Q_L}{A_c} \tag{B.6}$$

$$U_G = \frac{Q_G}{A_c} \tag{B.7}$$

Considering a one-dimensional approach, the variables are cross-sectional averaged. It follows:

$$J_L = U_L = \frac{Q_L}{A_c} \tag{B.8}$$

$$J_G = U_G = \frac{Q_G}{A_c} \tag{B.9}$$

Therefore, the phase velocities, in a one-dimensional approach, read as follows:

$$w_L = \frac{U_L}{(1-\varepsilon_G)} \tag{B.10}$$

$$w_G = \frac{U_G}{\varepsilon_G} \tag{B.11}$$

At this point, the relative velocity and the drift velocities are defined. The relative velocity between the phases, $w_{G\text{-}L}$, is defined as follows:

$$w_{G-L} = (w_G - w_L) = -w_{L-G} \tag{B.12}$$

Conversely, drift velocities ($w_{G->L}$) are defined as the difference between the phases velocities and the average, as follows:

$$w_{G->J} = w_G - J \tag{B.13}$$

$$w_{L->J} = w_L - J \tag{B.14}$$

Finally, the drift flux can be defined. The drift flux, represents the volumetric flux of one phase relative to a surface moving at the average velocity. For the gas and liquid phase it reads as follows:

$$J_{G->L} = \varepsilon_G (w_G - J) \tag{B.15}$$

$$J_{L->G} = (1-\varepsilon_G)(w_L - J) \tag{B.16}$$

Substituting Eq. (A.3) into Eq. (A.15) and using Eq. (A.2) (considering Eq. (A.8) and Eq. (A.9)), it follows, for the gas phase:

$$J_{G->L} = U_G - \varepsilon_G (U_L - U_G) = U_G(1-\varepsilon_G) - U_L\varepsilon_G \tag{B.17}$$

Similarly, for the liquid phase:

$$J_{G->L} = U_L\varepsilon_G - U_G(1-\varepsilon_G) \tag{B.18}$$

Therefore:

$$J_{G->L} = -J_{L->G} = J_T \tag{B.19}$$

Substituting for U_G and U_L in Eq. (B.18) by using Eqs. (B.10) and (B.11), we obtain a relation between the drift flux and the relative phase velocity:

$$J_{G->L} = J_T = \varepsilon_G(1-\varepsilon_G)(w_L - w_G) = \varepsilon_G(1-\varepsilon_G) w_{L-G} \tag{B.20}$$

References

Akita, K., Yoshida, F., 1973. Gas holdup and volumetric mass transfer coefficient in bubble columns. effects of liquid properties. Indust. Eng. Chem. Process Des. Dev. 12, 76–80.

Baawain, M.S., El-Din, M.G., Smith, D.W., 2007. Artificial neural networks modeling of ozone bubble columns: mass transfer coefficient, gas hold-up, and bubble size. Ozone Sci. Eng. 29, 343–352.

Beinhauer, R., 1971. Dynamic Measurement of the Relative Gas Contents in Bubble Columns By Means of X-ray Absorption. TU Berlin.

Besagni, G., Guédon, G., Inzoli, F., 2014. Experimental investigation of counter current air-water flow in a large diameter vertical pipe with inners. J. Phys. 547, 012024.

Besagni, G., Guédon, G.R., Inzoli, F., 2016a. Annular gap bubble column: experimental investigation and computational fluid dynamics modeling. J. Fluids Eng. 138, 011302.

Besagni, G., Inzoli, F., 2015. Influence of electrolyte concentration on holdup, flow regime transition and local flow properties in a large scale bubble column. J. Phys. 655.

Besagni, G., Inzoli, F., 2016a. Bubble size distributions and shapes in annular gap bubble column. Exp. Therm. Fluid Sci. 74, 27–48.

Besagni, G., Inzoli, F., 2016b. Comprehensive experimental investigation of counter-current bubble column hydrodynamics: holdup, flow regime transition, bubble size distributions and local flow properties. Chem. Eng. Sci. 146, 259–290.

Besagni, G., Inzoli, F., 2016c. Influence of internals on counter-current bubble column hydrodynamics: Holdup, flow regime transition and local flow properties. Chem. Eng. Sci. 145, 162–180.

Besagni, G., Inzoli, F., De Guido, G., Pellegrini, L.A., 2016b. Experimental investigation on the influence of ethanol on bubble column hydrodynamics. Chem. Eng. Res. Des. 112, 1–15.

Besagni, G., Inzoli, F., De Guido, G., Pellegrini, L.A., 2017. The dual effect of viscosity on bubble column hydrodynamics. Chem. Eng. Sci. 158, 509–538.

Bin, A.K., Duczmal, B., Machniewski, P., 2001. Hydrodynamics and ozone mass transfer in a tall bubble column. Chem. Eng. Sci. 56, 6233–6240.

Brooks, C.S., Paranjape, S.S., Ozar, B., Hibiki, T., Ishii, M., 2012. Two-group drift-flux model for closure of the modified two-fluid model. Int. J. Heat Fluid Flow 37, 196–208.

Craig, V.S.J., Ninham, B.W., Pashley, R.M., 1993. The effect of electrolytes on bubble coalescence in water. J. Phys. Chem. 97, 10192–10197.

de Bruijn, T.J.W., Chase, J.D., Dawson, W.H., 1988. Gas holdup in a two-phase vertical tubular reactor at high pressure. Can. J. Chem. Eng. 66, 330–333.

De Guido, G., Besagni, G., Inzoli, F., Pellegrini, L.A., 2016. New gas holdup data in large counter-current bubble columns. ICMF-2016 - 9th International Conference on Multiphase Flow.

Deschenes, L.A., Barrett, J., Muller, L.J., Fourkas, J.T., Mohanty, U., 1998. Inhibition of bubble coalescence in aqueous solutions. 1. Electrolytes. J. Phys. Chem. B 102, 5115–5119.

Firouzi, M., Howes, T., Nguyen, A.V., 2015. A quantitative review of the transition salt concentration for inhibiting bubble coalescence. Adv. Colloid Interface Science 222, 305–318.

Hai-Lang, Z., Shi-Jun, H., 1996. Viscosity and density of water+ sodium chloride+ potassium chloride solutions at 298.15 K. J. Chem. Eng. Data 41, 516–520. Haynes, W.M., 2014. CRC Handbook of Chemistry and Physics. CRC press.

Hills, J.H., 1976. The operation of a bubble column at high throughputs: I. gas holdup measurements. Chem. Eng. J. 12, 89–99.

Jin, H., Yang, S., He, G., Wang, M., Williams, R.A., 2010. The effect of gas-liquid counter-current operation on gas hold-up in bubble columns using electrical resistance tomography. J. Chem. Technol. Biotechnol. 85, 1278–1283.

Kastanek, F., Zahradnik, J., Kratochvil, J., Cermak, J., 1984. Modeling of large-scale bubble column reactors for non-ideal gas–liquid systems. Front. Chem. Reaction Eng. 1, 330–344.

Keitel, G., Onken, U., 1982. Inhibition of bubble coalescence by solutes in air/water dispersions. Chem. Eng. Sci. 37, 1635–1638.

Kitscha, J., Kocamustafaogullari, G., 1989. Breakup criteria for fluid particles. Int. J. Multiphase Flow 15, 573–588.

Krishna, R., Dreher, A.J., Urseanu, M.I., 20 0 0a. Influence of alcohol addition on gas hold-up in bubble columns: development of a scale up model. Int. Commun. Heat Mass Transfer 27, 465–472.

Krishna, R., Urseanu, M.I., Dreher, A.J., 2000b. Gas hold-up in bubble columns: influence of alcohol addition versus operation at elevated pressures. Chem. Eng. Process. 39, 371–378.

Krishna, R., Wilkinson, P.M., Van Dierendonck, L.L., 1991. A model for gas holdup in bubble columns incorporating the influence of gas density on flow regime transitions. Chem. Eng. Sci. 46, 2491–2496.

Lau, R., Peng, W., Velazquez-Vargas, L.G., Yang, G.Q., Fan, L.S., 2004. Gas-liquid mass transfer in high-pressure bubble columns. Ind. Eng. Chem. Res. 43, 1302–1311.

Leonard, C., Ferrasse, J.H., Boutin, O., Lefevre, S., Viand, A., 2015. Bubble column reactors for high pressures and high temperatures operation. Chem. Eng. Res. Des. 100, 391–421.

Lessard, R.R., Zieminski, S.A., 1971. Bubble coalescence and gas transfer in aqueous electrolytic solutions. Indust. Eng. Chem. Fundam. 10, 260–269.

Lucas, D., Krepper, E., Prasser, H.M., Manera, A., 2006. Investigations on the stability of the flow characteristics in a bubble column. Chem. Eng. Technol. 29, 1066–1072.

Lucas, D., Prasser, H.M., Manera, A., 2005. Influence of the lift force on the stability of a bubble column. Chem. Eng. Sci. 60, 3609–3619.

Lucas, D., Rzehak, R., Krepper, E., Ziegenhein, T., Liao, Y., Kriebitzsch, S., Apanasevich, P., 2015. A strategy for the qualification of multi-fluid approacheds for nuclear reactor safety. Nucl. Eng. Des.

Majumder, S.K., 2016. Hydrodynamics and Transport Processes of Inverse Bubbly Flow. Elsevier Inc.

Marrucci, G., Nicodemo, L., 1967. Coalescence of gas bubbles in aqueous solutions of inorganic electrolytes. Chem. Eng. Sci. 22, 1257–1265.

Montoya, G., Lucas, D., Baglietto, E., Liao, Y., 2016. A review on mechanisms and models for the churn-turbulent flow regime. Chem. Eng. Sci. 141, 86–103.

Mudde, R.F., Harteveld, W.K., van den Akker, H.E.A., 2009. Uniform flow in bubble columns. Indust. Eng. Chem. Res. 48, 148–158.

Nedeltchev, S., 2015. New methods for flow regime identification in bubble columns and fluidized beds. Chem. Eng. Sci. 137, 436–446.

Nguyen, P.T., Hampton, M.A. , Nguyen, A .V., Birkett, G.R., 2012. The influence of gas velocity, salt type and concentration on transition concentration for bubble coalescence inhibition and gas holdup. Chem. Eng. Res. Des. 90, 33–39.

Orvalho, S., Ruzicka, M.C., Drahos, J., 2009. Bubble column with electrolytes: gas holdup and flow regimes. Indust. Eng. Chem. Res. 48, 8237–8243.

Otake, T., Tone, S., Shinohara, K., 1981. Gas holdup in the bubble column with cocurrent and countercurrent gas-liquid flow. J. Chem. Eng. Jpn. 338–340.

Pagan, E., Williams, W.C., Kam, S., Waltrich, P.J., 2017. A simplified model for churn and annular flow regimes in small- and large-diameter pipes. Chem. Eng. Sci. 162, 309–321.

Patil, V.K., Joshi, J.B., Sharma, M.M., 1984. Sectionalised bubble column: gas hold-up and wall side solid—liquid mass transfer coefficient. Can. J. Chem. Eng. 62, 228–232.

Prince, M.J., Blanch, H.W., 1990. Transition electrolyte concentrations for bubble coalescence. AIChE J. 36, 1425–1429.

Reilly, I., Scott, D., Debruijn, T., MacIntyre, D., 1994. The role of gas phase momentum in determining gas holdup and hydrodynamic flow regimes in bubble column operations. Can. J. Chem. Eng. 72, 3–12.

Reilly, I.G., Scott, D.S., De Bruijn, T., Jain, A., Piskorz, J., 1986. A correlation for gas holdup in turbulent coalescing bubble columns. Can. J. Chem. Eng. 64, 705–717.

Ribeiro Jr., C.P., Mewes, D., 2007. The influence of electrolytes on gas hold-up and regime transition in bubble columns. Chem. Eng. Sci. 62, 4501–4509.

Richardson, J.F., Zaki, W.N., 1997. Sedimentation and fluidisation: part I. Chem. Eng. Res. Des. 75 (Supplement), S82–S100.

Rollbusch, P., Becker, M., Ludwig, M., Bieberle, A., Grünewald, M., Hampel, U., Franke, R., 2015a. Experimental investigation of the influence of column scale, gas density and liquid properties on gas holdup in bubble columns. Int. J. Multiphase Flow 75, 88–106.

Rollbusch, P., Bothe, M., Becker, M., Ludwig, M., Grünewald, M., Schlüter, M., Franke, R., 2015b. Bubble columns operated under industrially relevant conditions–current understanding of design parameters. Chem. Eng. Sci. 126, 660–678.

Ruzicka, M.C., Drahoš, J., Mena, P.C., Teixeira, J.A., 2003. Effect of viscosity on homogeneous–heterogeneous flow regime transition in bubble columns. Chem. Eng. J. 96, 15–22.

Ruzicka, M.C., Drahovs, J., Fialova, M., Thomas, N.H., 2001a. Effect of bubble column dimensions on flow regime transition. Chem. Eng. Sci. 56, 6117–6124.

Ruzicka, M.C., Vecer, M.M., Orvalho, S., Drahoš, J., 2008. Effect of surfactant on homogeneous regime stability in bubble column. Chem. Eng. Sci. 63, 951–967.

Ruzicka, M.C., Zahradník, J., Drahoš, J., Thomas, N.H., 2001b. Homogeneous–heterogeneous regime transition in bubble columns. Chem. Eng. Sci. 56, 4609–4626.

Rzehak, R., 2016. Modeling of mass-transfer in bubbly flows encompassing different mechanisms. Chem. Eng. Sci. 151, 139–143.

Sangnimnuan, A., Prasad, G.N., Agnew, J.B., 1984. Gas hold-up and backmixing in a bubble-column reactor under coal-hydroliquefaction conditions. Chem. Eng. Commun. 25, 193–212.

Sarrafi, A., Müller-Steinhagen, H., Smith, J.M., Jamialahmadi, M., 1999. Gas holdup in homogeneous and heterogeneous gas—liquid bubble column reactors. Can. J. Chem. Eng. 77, 11–21.

Sasaki, S., Hayashi, K., Tomiyama, A., 2016. Effects of liquid height on gas holdup in air–water bubble column. Exp. Thermal Fluid Sci. 72, 67–74.

Sasaki, S., Uchida, K., Hayashi, K., Tomiyama, A., 2017. Effects of column diameter and liquid height on gas holdup in air-water bubble columns. Exp. Thermal Fluid Sci. 82, 359–366.

Schumpe, A., Grund, G., 1986. The gas disengagement technique for studying gas holdup structure in bubble columns. Can. J. Chem. Eng. 64, 891–896.

Shah, Y.T., Joseph, S., Smith, D.N., Ruether, J.A., 1985. On the behavior of the gas phase in a bubble column with ethanol-water mixtures. Indust. Eng. Chem. Process Des. Dev. 24, 1140–1148.

Shah, Y.T., Kelkar, B.G., Godbole, S.P., Deckwer, W.D., 1982. Design parameters estimations for bubble column reactors. AIChE J. 28, 353–379.

Shaikh, A., Al-Dahhan, M., 2013. Scale-up of bubble column reactors: a review of current state-of-the-art. Indust. Eng. Chem. Res. 52, 8091–8108.

Sharaf, S., Zednikova, M., Ruzicka, M.C., Azzopardi, B.J., 2015. Global and local hydrodynamics of bubble columns–effect of gas distributor. Chem. Eng. J. 288, 489–504.

Shawaqfeh, A.T., 2003. Gas holdup and liquid axial dispersion under slug flow conditions in gas–liquid bubble column. Chem. Eng. Process. 42, 767–775.

Shawkat, M.E., Ching, C.Y., 2011. Liquid turbulence kinetic energy budget of co-current bubbly flow in a large diameter vertical pipe. J. Fluids Eng. 133, 091303.

Takagi, S., Matsumoto, Y., 2011. Surfactant effects on bubble motion and bubbly flows. Ann. Rev. Fluid Mech. 43, 615–636.

Takagi, S., Ogasawara, T., Matsumoto, Y., 2008. The effects of surfactant on the multiscale structure of bubbly flows. Philos. Trans. R. Soc. A 366, 2117–2129.

Thorat, B.N., Shevade, A.V., Bhilegaonkar, K.N., Aglawe, R.H., Parasu Veera, U., Thakre, S.S., Pandit, A.B., Sawant, S.B., Joshi, J.B., 1998. Effect of Sparger Design and height to diameter ratio on fractional gas hold-up in bubble columns. Chem. Eng. Res. Des. 76, 823–834.

Tomiyama, A., Tamai, H., Zun, I., Hosokawa, S., 2002. Transverse migration of single bubbles in simple shear flows. Chem. Eng. Sci. 57, 1849–1858.

Voigt, J., Schügerl, K., 1979. Absorption of oxygen in countercurrent multistage bubble columns—I aqueous solutions with low viscosity. Chem. Eng. Sci. 34, 1221–1229.

Wallis, G.B., 1969. One-Dimensional Two-Phase Flow. McGraw-Hill, New York.

Weissenborn, P.K., Pugh, R.J., 1996. Surface tension of aqueous solutions of electrolytes: relationship with ion hydration, oxygen solubility, and bubble coalescence. J. Colloid Interface Sci. 184, 550–563.

Wilkinson, P.M., Spek, A.P., van Dierendonck, L.L., 1992. Design parameters estimation for scale-up of high-pressure bubble columns. AIChE J. 38, 544–554.

Xue, J., Al-Dahhan, M., Dudukovic, M.P., Mudde, R.F., 2008. Bubble velocity, size, and interfacial area measurements in a bubble column by four-point optical probe. AIChE J. 54, 350–363.

Yamaguchi, K., Yamazaki, Y., 1982. Characteristics of counter current gas-liquid two-phase flow in vertical tubes. J. Nucl. Sci. Technol. 19, 985–996.

Yang, G.Q., Fan, L.S., 2003. Axial liquid mixing in high-pressure bubble columns. AIChE J. 49, 1995–2008.

Yang, J.H., Yang, J.-I., Kim, H.-J., Chun, D.H., Lee, H.-T., Jung, H., 2010. Two regime transitions to pseudo-homogeneous and heterogeneous bubble flow for various liquid viscosities. Chem. Eng. Process. 49, 1044–1050.

Yoshida, F., Akita, K., 1965. Performance of gas bubble columns: Volumetric liquid-phase mass transfer coefficient and gas holdup. AIChE J. 11, 9–13.

Youssef Ahmed, A., Al-Dahhan Muthanna, H., Dudukovic Milorad, P., 2013. Bubble columns with internals: a review. Int. J. Chem. Reactor Eng. 169.

Zahradník, J., Fialová, M., Linek, V., 1999. The effect of surface-active additives on bubble coalescence in aqueous media. Chem. Eng. Sci. 54, 4757–4766.

Zahradník, J., Fialová, M., Ruzicka, M., Drahoš, J., Kastanek, F., Thomas, N.H. , 1997. Duality of the gas–liquid flow regimes in bubble column reactors. Chem. Eng. Sci. 52, 3811–3826.

Ziegenhein, T., Rzehak, R., Lucas, D., 2015. Transient simulation for large scale flow in bubble columns. Chem. Eng. Sci. 122, 1–13.

Zuber, N., Findlay, J.A., 1965. Average volumetric concentration in two-phase flow systems. J. Heat Transfer 87, 453–468.